Therefore, some off-target effects exerted through RISC cleavage may be attenuated by lowering the siRNA concentration.

mRNA that has a 3′ untranslated region containing a sequence complementary to nucleotide 2–7 of the 5′ end of the guide strand, analogous to the seed region of miRNA, can be a collateral target for siRNA-mediated translation inhibition.[20–22] Those studies also suggested that all siRNAs potentially possess miRNA-like activities. To minimize such off-target effects, complementarity between the guide strand and human genes should be carefully analyzed. Chemical modifications of siRNAs, such as a 2′*O*-methyl ribose modification, have been reported to reduce the miRNA-like off-target effect without compromising RNAi activity.[42]

siRNAs can also exert unintended effects through IFN-I and inflammatory cytokine production. Receptors of siRNAs for immunostimulation include double-stranded RNA-dependent protein kinase (PKR) and toll-like receptors (TLRs), such as TLR3, TLR7 and TLR8. siRNAs with sequences of 5′-GUCCUUCAA-3′, 5′-UGUGU-3′ and 5′-UGUCU-3′ have been shown to stimulate mouse TLR7 and, most likely, human TLR8.[23,24] Among the E6 and E7 siRNAs selected in our study, siRNA 497 contained the 5′-UGUCU-3′ sequence. Activation of TRLs may be bypassed by delivery of an siRNA in a cholesterol-conjugated[43] or atelocollagen-complexed form,[44] as well as following chemical modification of the RNA backbone.[45]

The mechanism by which the present siRNAs exhibited their off-target effects on HPV16− cells was not revealed. However, nonspecific growth suppression of three of the siRNAs (497, 573, 752) was significantly improved without compromising their strong growth suppression of HPV16+ cells by reducing the siRNA concentration to as low as 1 nM. To further improve the off-target effect, we are now working on backbone modification of these siRNAs, which has been reported to attenuate miRNA-like activity and cytokine response.[42,45,46]

miRNA has been implicated in diverse regulation pathways, including control of cell differentiation, apoptosis, cell proliferation and organ development. Long-term use of a high dose of siRNA might disturb these normal functions of miRNA by saturating the limited source of RNAi machinery. Therefore, it is important to administer a minimal dose of synthetic siRNA with high RNAi activity. A molecular abundance of human miRNA in HeLa cells has been reported.[47] The calculated intracellular concentrations of different miRNAs, including miR-22, miR-16, let-7 and miR-21, in HeLa cells ranges from about 0.1 to 2 nM, when assuming that the cell volume is about 10 pl. Therefore, administration of E6 and E7 siRNAs that do not exceed an intracellular concentration of 2 nM should safely exert an antitumor effect without disturbing endogenous RNAi.

In the present experiments, we identified three new siRNAs (497, 573, 752) that possessed high RNAi activities toward E6 and E7 expression, and whose growth inhibition effects were potent and specific to HPV16+ cancer cells. Furthermore, the sequences of those siRNAs showed full complementarity with all HPV16 classes and subclasses. We also performed a literature search to determine if the siRNAs were compatible with E6 and E7 variants found in patient samples from various countries (total 991 cases).[32–37] Three variants were found in the same series of patients from Hong Kong (255 patients),[35] with E6(517G), in which thymine at nt 517, located at the 5′ end of the 497 guide strand, was changed to guanine, found in three patients, E7(757T), which carried thymine instead of cytosine at nt 757, found in one patient and E7(760c), which contained thymine instead of cytosine at nt 760, found in seven patients (3.1%). These variants were not seen in patients from other areas. Thus, siRNA 497, 573 and 752 are considered to be compatible with most HPV16 variants.

Deregulation of E6 and E7 expression is a necessary cause of malignant transformation, and additional genetic alterations accumulate before progression to carcinoma development. Studies using antisense oligo-DNA, ribozymes, transcriptional suppression by forced E2 expression, and siRNAs have revealed that inhibition of E6 and E7 expression is sufficient to cause growth suppression of HPV-related cancer cells.[7–9,12–18,48] In the present study, E6 and E7 siRNA-induced growth suppression was associated with morphological and cytochemical characteristics of cellular senescence. Our results are consistent with other studies, which also demonstrated that downregulation of E6 and E7 causes *in vitro* and *in vivo* growth suppression, as well as cellular senescence.[15,16,48] Induction of senescence might be caused by reactivation of PML, which has been shown to be a mediator of senescence and a target of E7.[6] Recently, human fibroblasts immortalized by a temperature sensitive SV40 large T antigen were reported to undergo irreversible senescence by a reactivated $p16^{INK4a}$/Rb pathway after incubation at a nonpermissive temperature for a specific period of time.[49] The functional similarity between SV40 large T antigen and hrHPV E6E7 suggests that siRNA-mediated senescence might be irreversible.

Infection with hrHPV causes intraepithelial precancerous lesions in the cervix, termed cervix intraepithelial neoplasia (CIS).[50] High-grade lesions (CIS grade 3) express deregulated hrHPV oncogenes and eventually develop into invasive cervical cancer after a long latency without spontaneous regression. Downregulation of the virus oncogenes using an siRNA could reverse the neoplastic phenotype and also prevent E7-induced genetic alterations. In hrHPV-infected lesions, replication of HPVs relies on E7 expression.[5] Thus, an siRNA targeting E7 may be able to inhibit virus replication as well as propagation. CIS lesions exist within epithelium and are easily accessible.[51] Furthermore, local siRNA administration could help to avoid its hazardous systemic off-target effects. Therefore, we consider such lesions to be ideal targets of RNAi therapy.

The US Food and Drug Administration (FDA) approved a preventive HPV vaccine for immunization of women between 9 and 26 years of age, with a second

vaccine now being tested. These HPV vaccines will eventually reduce the incidence rates of viral infection and cervical cancer. However, there are currently no effective therapies for individuals infected with HPV and a small fraction of those patients will develop cancer in a decade or two.[50] Notably, immunosuppressed patients such as organ transplant recipients and HIV-infected patients, whose response to an HPV vaccine is unknown, have greater propensity for cervical cancer and anal cancer.[52,53] It is also unclear how long the protection provided by the HPV vaccines will last. Therefore, RNAi therapy using potent and specific siRNAs will benefit patients infected with HPV. Also, in parallel with HPV vaccination, RNAi therapy may speed up the reduction in rates of incidence of HPV infection and cervical cancer.

Acknowledgements

We thank Dr Hideki Matsui and Dr Kazuhito Tomizawa (Okayama University) for their helpful discussion and suggestions. This work was supported in part by Grants-in-aid for Scientific Research (C) from Japan Society for the Promotion of Science [15591749 (MY), 19592169 (KY)].

References

1 Bosch FX, de Sanjose S. Chapter 1: human papillomavirus and cervical cancer—burden and assessment of causality. *J Natl Cancer Inst Monogr* 2003; **31**: 3–13.
2 zur Hausen H. Papillomaviruses causing cancer: evasion from host-cell control in early events in carcinogenesis. *J Natl Cancer Inst* 2000; **92**: 690–698.
3 Longworth MS, Laimins LA. Pathogenesis of human papillomaviruses in differentiating epithelia. *Microbiol Mol Biol Rev* 2004; **68**: 362–372.
4 Munger K, Baldwin A, Edwards KM, Hayakawa H, Nguyen CL, Owens M *et al*. Mechanisms of human papillomavirus-induced oncogenesis. *J Virol* 2004; **78**: 11451–11460.
5 Flores ER, Allen-Hoffmann BL, Lee D, Lambert PF. The human papillomavirus type 16 E7 oncogene is required for the productive stage of the viral life cycle. *J Virol* 2000; **74**: 6622–6631.
6 Bischof O, Nacerddine K, Dejean A. Human papillomavirus oncoprotein E7 targets the promyelocytic leukemia protein and circumvents cellular senescence via the Rb and p53 tumor suppressor pathways. *Mol Cell Biol* 2005; **25**: 1013–1024.
7 Venturini F, Braspenning J, Homann M, Gissmann L, Sczakiel G. Kinetic selection of HPV 16 E6/E7-directed antisense nucleic acids: anti-proliferative effects on HPV 16-transformed cells. *Nucleic Acids Res* 1999; **27**: 1585–1592.
8 Alvarez-Salas LM, Cullinan AE, Siwkowski A, Hampel A, DiPaolo JA. Inhibition of HPV-16 E6/E7 immortalization of normal keratinocytes by hairpin ribozymes. *Proc Natl Acad Sci USA* 1998; **95**: 1189–1194.
9 Chen Z, Kamath P, Zhang S, St John L, Adler-Storthz K, Shillitoe EJ. Effects on tumor cells of ribozymes that cleave the RNA transcripts of human papillomavirus type 18. *Cancer Gene Ther* 1996; **3**: 18–23.
10 Elbashir SM, Harborth J, Lendeckel W, Yalcin A, Weber K, Tuschl T. Duplexes of 21-nucleotide RNAs mediate RNA interference in cultured mammalian cells. *Nature* 2001; **411**: 494–498.
11 Caplen NJ, Parrish S, Imani F, Fire A, Morgan RA. Specific inhibition of gene expression by small double-stranded RNAs in invertebrate and vertebrate systems. *Proc Natl Acad Sci USA* 2001; **98**: 9742–9747.
12 Jiang M, Milner J. Selective silencing of viral gene expression in HPV-positive human cervical carcinoma cells treated with siRNA, a primer of RNA interference. *Oncogene* 2002; **21**: 6041–6048.
13 Yoshinouchi M, Yamada T, Kizaki M, Fen J, Koseki T, Ikeda Y *et al*. *In vitro* and *in vivo* growth suppression of human papillomavirus 16-positive cervical cancer cells by E6 siRNA. *Mol Ther* 2003; **8**: 762–768.
14 Butz K, Ristriani T, Hengstermann A, Denk C, Scheffner M, Hoppe-Seyler F. siRNA targeting of the viral E6 oncogene efficiently kills human papillomavirus-positive cancer cells. *Oncogene* 2003; **22**: 5938–5945.
15 Hall AH, Alexander KA. RNA interference of human papillomavirus type 18 E6 and E7 induces senescence in HeLa cells. *J Virol* 2003; **77**: 6066–6069.
16 Putral LN, Bywater MJ, Gu W, Saunders NA, Gabrielli BG, Leggatt GR *et al*. RNA interference against human papillomavirus oncogenes in cervical cancer cells results in increased sensitivity to cisplatin. *Mol Pharmacol* 2005; **68**: 1311–1319.
17 Niu XY, Peng ZL, Duan WQ, Wang H, Wang P. Inhibition of HPV 16 E6 oncogene expression by RNA interference *in vitro* and *in vivo*. *Int J Gynecol Cancer* 2006; **16**: 743–751.
18 Gu W, Putral L, Hengst K, Minto K, Saunders NA, Leggatt G *et al*. Inhibition of cervical cancer cell growth *in vitro* and *in vivo* with lentiviral-vector delivered short hairpin RNA targeting human papillomavirus E6 and E7 oncogenes. *Cancer Gene Ther* 2006; **13**: 1023–1032.
19 Kuner R, Vogt M, Sultmann H, Buness A, Dymalla S, Bulkescher J *et al*. Identification of cellular targets for the human papillomavirus E6 and E7 oncogenes by RNA interference and transcriptome analyses. *J Mol Med* 2007; **85**: 1253–1262.
20 Jackson AL, Bartz SR, Schelter J, Kobayashi SV, Burchard J, Mao M *et al*. Expression profiling reveals off-target gene regulation by RNAi. *Nat Biotechnol* 2003; **21**: 635–637.
21 Lin X, Ruan X, Anderson MG, McDowell JA, Kroeger PE, Fesik SW *et al*. siRNA-mediated off-target gene silencing triggered by a 7 nt complementation. *Nucleic Acids Res* 2005; **33**: 4527–4535.
22 Jackson AL, Burchard J, Schelter J, Chau BN, Cleary M, Lim L *et al*. Widespread siRNA 'off-target' transcript silencing mediated by seed region sequence complementarity. *RNA* 2006; **12**: 1179–1187.
23 Hornung V, Guenthner-Biller M, Bourquin C, Ablasser A, Schlee M, Uematsu S *et al*. Sequence-specific potent induction of IFN-alpha by short interfering RNA in plasmacytoid dendritic cells through TLR7. *Nat Med* 2005; **11**: 263–270.
24 Judge AD, Sood V, Shaw JR, Fang D, McClintock K, MacLachlan I. Sequence-dependent stimulation of the mammalian innate immune response by synthetic siRNA. *Nat Biotechnol* 2005; **23**: 457–462.
25 Haley B, Zamore PD. Kinetic analysis of the RNAi enzyme complex. *Nat Struct Mol Biol* 2004; **11**: 599–606.
26 Ui-Tei K, Naito Y, Takahashi F, Haraguchi T, Ohki-Hamazaki H, Juni A *et al*. Guidelines for the selection of

highly effective siRNA sequences for mammalian and chick RNA interference. *Nucleic Acids Res* 2004; **32**: 936–948.
27 Naito Y, Yamada T, Ui-Tei K, Morishita S, Saigo K. siDirect: highly effective, target-specific siRNA design software for mammalian RNA interference. *Nucleic Acids Res* 2004; **32**: W124–W129.
28 Kanda T, Furuno A, Yoshiike K. Human papillomavirus type 16 open reading frame E7 encodes a transforming gene for rat 3Y1 cells. *J Virol* 1988; **62**: 610–613.
29 Smotkin D, Prokoph H, Wettstein FO. Oncogenic and nononcogenic human genital papillomaviruses generate the E7 mRNA by different mechanisms. *J Virol* 1989; **63**: 1441–1447.
30 Schwarz DS, Hutvagner G, Du T, Xu Z, Aronin N, Zamore PD. Asymmetry in the assembly of the RNAi enzyme complex. *Cell* 2003; **115**: 199–208.
31 Khvorova A, Reynolds A, Jayasena SD. Functional siRNAs and miRNAs exhibit strand bias. *Cell* 2003; **115**: 209–216.
32 Matsumoto K, Yoshikawa H, Nakagawa S, Tang X, Yasugi T, Kawana K *et al.* Enhanced oncogenicity of human papillomavirus type 16 (HPV16) variants in Japanese population. *Cancer Lett* 2000; **156**: 159–165.
33 Hu X, Pang T, Guo Z, Ponten J, Nister M, Bernard Afink G. Oncogene lineages of human papillomavirus type 16 E6, E7 and E5 in preinvasive and invasive cervical squamous cell carcinoma. *J Pathol* 2001; **195**: 307–311.
34 Zehbe I, Tachezy R, Mytilineos J, Voglino G, Mikyskova I, Delius H *et al.* Human papillomavirus 16 E6 polymorphisms in cervical lesions from different European populations and their correlation with human leukocyte antigen class II haplotypes. *Int J Cancer* 2001; **94**: 711–716.
35 Chan PK, Lam CW, Cheung TH, Li WW, Lo KW, Chan MY *et al.* Human papillomavirus type 16 intratypic variant infection and risk for cervical neoplasia in southern China. *J Infect Dis* 2002; **186**: 696–700.
36 Kammer C, Tommasino M, Syrjanen S, Delius H, Hebling U, Warthorst U *et al.* Variants of the long control region and the E6 oncogene in European human papillomavirus type 16 isolates: implications for cervical disease. *Br J Cancer* 2002; **86**: 269–273.
37 Tornesello ML, Duraturo ML, Salatiello I, Buonaguro L, Losito S, Botti G *et al.* Analysis of human papillomavirus type-16 variants in Italian women with cervical intraepithelial neoplasia and cervical cancer. *J Med Virol* 2004; **74**: 117–126.
38 Brown KM, Chu CY, Rana TM. Target accessibility dictates the potency of human RISC. *Nat Struct Mol Biol* 2005; **12**: 469–470.
39 Schubert S, Grunweller A, Erdmann VA, Kurreck J. Local RNA target structure influences siRNA efficacy: systematic analysis of intentionally designed binding regions. *J Mol Biol* 2005; **348**: 883–893.
40 Overhoff M, Alken M, Far RK, Lemaitre M, Lebleu B, Sczakiel G *et al.* Local RNA target structure influences siRNA efficacy: a systematic global analysis. *J Mol Biol* 2005; **348**: 871–881.
41 Sledz CA, Holko M, de Veer MJ, Silverman RH, Williams BR. Activation of the interferon system by short-interfering RNAs. *Nat Cell Biol* 2003; **5**: 834–839.
42 Jackson AL, Burchard J, Leake D, Reynolds A, Schelter J, Guo J *et al.* Position-specific chemical modification of siRNAs reduces 'off-target' transcript silencing. *RNA* 2006; **12**: 1197–1205.
43 Soutschek J, Akinc A, Bramlage B, Charisse K, Constien R, Donoghue M *et al.* Therapeutic silencing of an endogenous gene by systemic administration of modified siRNAs. *Nature* 2004; **432**: 173–178.
44 Takeshita F, Minakuchi Y, Nagahara S, Honma K, Sasaki H, Hirai K *et al.* Efficient delivery of small interfering RNA to bone-metastatic tumors by using atelocollagen *in vivo*. *Proc Natl Acad Sci USA* 2005; **102**: 12177–12182.
45 Kariko K, Buckstein M, Ni H, Weissman D. Suppression of RNA recognition by Toll-like receptors: the impact of nucleoside modification and the evolutionary origin of RNA. *Immunity* 2005; **23**: 165–175.
46 Morrissey DV, Lockridge JA, Shaw L, Blanchard K, Jensen K, Breen W *et al.* Potent and persistent *in vivo* anti-HBV activity of chemically modified siRNAs. *Nat Biotechnol* 2005; **23**: 1002–1007.
47 Lim LP, Lau NC, Weinstein EG, Abdelhakim A, Yekta S, Rhoades MW *et al.* The microRNAs of *Caenorhabditis elegans*. *Genes Dev* 2003; **17**: 991–1008.
48 DeFilippis RA, Goodwin EC, Wu L, DiMaio D. Endogenous human papillomavirus E6 and E7 proteins differentially regulate proliferation, senescence, and apoptosis in HeLa cervical carcinoma cells. *J Virol* 2003; **77**: 1551–1563.
49 Takahashi A, Ohtani N, Yamakoshi K, Iida S, Tahara H, Nakayama K *et al.* Mitogenic signalling and the $p16I^{INK4a}$-Rb pathway cooperate to enforce irreversible cellular senescence. *Nat Cell Biol* 2006; **8**: 1291–1297.
50 Snijders PJ, Steenbergen RD, Heideman DA, Meijer CJ. HPV-mediated cervical carcinogenesis: concepts and clinical implications. *J Pathol* 2006; **208**: 152–164.
51 Palliser D, Chowdhury D, Wang QY, Lee SJ, Bronson RT, Knipe DM *et al.* An siRNA-based microbicide protects mice from lethal herpes simplex virus 2 infection. *Nature* 2006; **439**: 89–94.
52 Koshiol JE, Schroeder JC, Jamieson DJ, Marshall SW, Duerr A, Heilig CM *et al.* Time to clearance of human papillomavirus infection by type and human immunodeficiency virus serostatus. *Int J Cancer* 2006; **119**: 1623–1629.
53 Palefsky J. Human papillomavirus-associated malignancies in HIV-positive men and women. *Curr Opin Oncol* 1995; **7**: 437–441.

Supplementary Information accompanies the paper on Cancer Gene Therapy website (htttp://www.nature.com/cgt)

ELSEVIER

Experimental Hematology

Experimental Hematology 36 (2008) 37–50

Mutated D4-guanine diphosphate–dissociation inhibitor is found in human leukemic cells and promotes leukemic cell invasion

Yuji Nakata[a,b,d], Kensuke Kondoh[a,b,e], Sachiko Fukushima[a], Akinori Hashiguchi[a], Wenlin Du[a], Mutsumi Hayashi[a,b], Jun-ichiroh Fujimoto[c], Jun-ichi Hata[a,c], and Taketo Yamada[a]

[a]*Department of Pathology and* [b]*Department of Pediatrics, Keio University School of Medicine, Tokyo, Japan;* [c]*National Center for Child Health and Development, Tokyo, Japan;* [d]*Department of Medicine, Division Hematology/Oncology, University of Pennsylvania, Philadelphia, Pa., USA;* [e]*Department of Pediatrics, St. Marianna University School of Medicine, Kanagawa, Japan*

(Received 20 December 2006; revised 23 July 2007; accepted 13 August 2007)

Objective. **Rho GTPase may be involved in human cancer invasion via the augmentation of cell motility and adhesion. We report on two point mutations of the D4-guanine diphosphate (GDP)–dissociation inhibitor (GDI) gene, one of the Rho-GDIs, which were found in a human leukemic cell line, Reh, and the mutated D4-GDI functions as an accelerator of leukemic cell invasion.**

Material and Methods. **We investigated the altered activity of GDP dissociation by mutated (mt) D4-GDI and the functions of this mt and wild-type (wt) D4-GDI in invasion. The mice inoculated with wt or mt D4-GDI vector–transfected Raji cells were observed and examined pathologically. Adhesiveness and cell motility of wt or mt D4-GDI vector–transfected Raji cells were examined. Finally, it was examined whether Rho activation was changed by mutation of D4-GDI under the condition of Rho-GDI knockdown.**

Results. **Two point mutations of the D4-GDI gene were found in Reh cells. The region of mutations is conserved among members of the Rho-GDI family at the amino acid level. D4-GDI with two mutations (V68L and V69A) functioned in a dominant negative manner in the inhibition of GDP dissociation from Rho. Severe combined immune-deficient mice inoculated with Raji cells developed hemiparalysis. The Raji cells were present in bone marrow and peripheral blood, and hepatic invasion was observed in 20% of the mice. Mice inoculated with wt D4-GDI vector–transfected Raji cells (wt D4) showed later paralysis and none developed hepatic invasion. Mice inoculated with mt D4-GDI–transfected Raji cells (mt D4) showed a 5-day reduction in the time to paraplegia and death. In addition, hepatic invasion was evident in 80% of mice transplanted with mt D4 cells. There were no differences in growth rates and amounts of guanine triphosphate (GTP)–bound Rho, cdc42, or Rac among all clones, however, GTP-bound Rho in mt D4 clone with short hairpin RNA (shRNA) vector for Rho-GDI knockdown was increased compared with wt D4 clone with shRNA vector for Rho-GDI knockdown. The mt D4 cells showed an augmentation of adhesiveness and cell motility. On the other hand, wt D4 cells showed a decreased ability of cell motility.**

Conclusion. **These results suggest the mutated D4-GDI functions as a dominant negative molecule against the wt D4-GDI and accelerates invasion via regulation of cytoskeletal machinery.** © **2008 ISEH - Society for Hematology and Stem Cells. Published by Elsevier Inc.**

Human leukemia progression is a process by which leukemic cells acquire more malignant properties, such as invasiveness. We previously established in vivo experimental systems of human leukemia invasion using severe combined immune-deficient (SCID) mice and reported that Rho activation augmented human leukemic cells invasion and changed the pattern of organs targeted by leukemic cells through the acceleration of leukemic cell adhesion [1].

The Rho, Rac, and Cdc 42 GTPases belong to the small guanine triphosphate (GTP)–binding protein family, a part of the Ras superfamily, and regulate various actin filament–dependent cell functions, such as cell adhesion, cell

Dr. Fukushima's current address: Department of Dermatology, Kanazawa University School of Medicine, Kanazawa, Japan.

Offprint requests to: Taketo Yamada, M.D., Department of Pathology, Keio University School of Medicine, 35 Shinano-machi, Shinjuku-ku, Tokyo 160-8582, Japan; E-mail: taketo@sc.itc.keio.ac.jp

0301-472X/08 $–see front matter.
doi: 10.1016/j.exphem.2007.08.023

motility, and cytokinesis [2–5], as well as certain gene expressions [6]. These GTPases are active only in GTP-bound states and the exchange of GTP and guanine diphosphate (GDP) is strictly regulated by three types of regulatory proteins; GDP dissociation stimulators (GDS), GDP dissociation inhibitors (GDI), and GTPase activating proteins (GAP). Some GDS and GAP from the Rho family and three Rho GDIs have been isolated [7]. D4-GDI, one of the Rho GDIs, is preferentially expressed in hematopoietic cells, and Rho-GDIγ is expressed in the brain, lungs, kidneys, testes, and pancreas, while Rho-GDI is ubiquitously expressed in all mammalian organs [8–10]. Rho-GDI binds the majority of Rho-family GTPases in the cytoplasm, maintaining Rho in an inactive form in which it cannot interact with effecter targets or other regulatory proteins [11]. On the other hand, Rho-GDI also associated weakly with the GTP-bound forms of Rho, Rac, and Cdc42 [12,13]. This weak interaction resulted in an inhibition of the intrinsic and GAP-stimulated GTPase activities of the Rho GTPases. Thus, Rho-GDI appears to be a molecule capable of blocking the GTP binding/GTPase cycle at two points: at the GDP–GTP exchange step and the GTP hydrolytic step. Further studies demonstrated that Rho-GDI associates with a Rho-GDI displacement factor from the ERM family, which consists of ezrin, radixin, and moesin. ERM interacts with both an adhesion molecule—CD44—and F-actin, resulting in association of the actin cytoskeleton with the plasma membrane [14]. D4-GDI has been identified as a Rho-GDI–like protein that is approximately 68% homologous with Rho-GDI, and is preferentially expressed at very high levels in hematopoietic cells, including erythroid, granulocytic, monocytic, and lymphoid cells [8]. In another report, expression of D4-GDI in lymphocytes was emphasized and D4-GDI was named Ly-GDI [9]. The inhibitory effect of D4-GDI on GDP dissociation was specific for Rho, but not Ras or Rap [8]. Like other Rho-GDIs, D4-GDI was postulated to bind and inhibit Rho GTPases. However, much yet remains to characterize the specificity of D4-GDI [15,16].

D4-GDI has been reported to be a substrate of the apoptosis protease CPP32. D4-GDI was rapidly truncated to a 23-kDa fragment in Jurkat cells with kinetics that parallel the onset of apoptosis following Fas cross-linking with agonistic antibody or treatment with staurosporine [17]. Furthermore, Krieser et al. [18] showed that a cleaved 26-kDa fragment derived from D4-GDI resided in the cytoplasm of undamaged cells, whereas after cleavage by CPP32, the 22-kDa form of D4-GDI translocated to the nucleus [18]. These lines of evidence suggest that D4-GDI is involved in cell-shape alterations and/or changes in cell fragmentation during leukocyte apoptosis.

A number of Ras gene mutations have been found in a wide variety of human malignant tumors, including leukemias and lymphomas [19]. Point mutations in Ras cause decreased GTPase activity and may transform in some leukemic cells. Rho, a member of the Ras family, has not been associated with transformation, and no Rho mutations have been detected in human malignant tumors to date [20]. However, it has been reported that some regulatory proteins for Rho GTPases, dbl, tiam1, and vav, are reportedly associated with tumor development [7,21,22]. The Dbl oncogene was originally discovered because of its ability to induce focus formation and tumorigenicity when expressed in NIH-3T3 cells [23]. Tiam, however, was first identified as an invasion-inducing gene using proviral tagging in combination with in vitro selection for invasiveness [24]. Furthermore, the Rho family of small GTPases, including Rac, Cdc42, and Rho, has been implicated in the regulation of many aspects of cancer cell motility and invasion, including cell polarity, cytoskeletal organization, and transduction of signals from the extracellular environment [25–28].

In this study, we identified two point mutations of the D4-GDI gene in a human B-cell leukemia cell line, Reh, and analyzed the functions of the mutated (mt) D4-GDI in vitro and in vivo employing an experimental system consisting of human leukemic cell invasion in SCID mice.

Materials and methods

Human leukemic cells and cell culture

Two acute lymphoblastic leukemia cell lines (Reh and HPB-ALL) and three Burkitt's lymphoma cell lines (Raji [ATCC, CCL-86], Ramos [ATCC, CRL-1923], and Daudi [ATCC, CCL-213]) were examined. The Reh cell line was established from a girl with a common form of acute lymphoblastic leukemia [29]. This cell line is known to be accompanied by the TEL-AML1 fusion gene due to chromosomal translocation [30]. We used reverse transcriptase polymerase chain reaction (RT-PCR) to confirm that our Reh cells expressed mRNA derived from the TEL-AML1 fusion gene (data not shown). The Raji cell line was derived from Burkitt's lymphoma. The HPB-ALL cell line was derived from a pediatric T-cell leukemia [31]. Cells were cultured in the presence of 5% CO_2 at 37°C using RPMI-1640 medium supplemented with 10% fetal bovine serum. Normal human peripheral blood lymphocytes from healthy Japanese men were also examined with informed consent.

RT-PCR and DNA sequencing

Total RNA was extracted from each sample (5–10 × 10^6 cells) using ISOGEN (Nippon Gene, Toyama, Japan). RNA was reverse-transcribed into first strand cDNA using a First-Strand cDNA Synthesis Kit (Amersham-Pharmacia Biotech, Buckinghamshire, UK). D4-GDI cDNA was isolated by PCR amplification from first-strand cDNA using the N-terminal primer (5′-TAAATA GATCAGAATGACTGAA-3′) and the C-terminal primer (5′-AGAATTCTTCCA AGGTGGCAA-3′). PCR was performed in 10 mM Tris-HCl (pH 9.0), 2.0 mM $MgCl_2$, 50 mM KCl, 0.2 mM each deoxyribonucleoside triphosphate, and 0.5 μM each PCR primer using Taq DNA Polymerase (Toyobo, Tokyo, Japan). Thirty cycles were run with denaturation at 94°C for 60 seconds, annealing at 55°C for 60 seconds, and extension at 72°C for 60

seconds. RT-PCR products were cloned into a pGEM-T vector (Promega, Madison, WI, USA), and analyzed with a Thermo Sequenase fluorescent-labeled primer cycle sequencing kit (Amersham-Pharmacia Biotech) using T7 and Sp6 fluorescent primer and a DNA sequencer (MegaBase 1000, Molecular Dynamics, Sunnyvale, CA, USA). The fluorescent primers used for sequencing were forward, 5′-GTCGCAGGAA ATGGACA AAGAT-3′ and reverse 5′-TCCAGTAA GGTCCATG GTGATT-3′.

Sequences of genomic D4-GDI DNA

DNA was prepared from Reh cells by standard methods with sodium dodecyl sulfate–proteinase K [32]. A portion of the D4-GDI gene that included the mutations was amplified using the N-terminal primer (5′-CACCACAGAAGTCCCTGAAAGA-3′) and the C-terminal primer (5′-TCCA GTAAGGTCCATGGT GATT-3′). PCR products were cloned into a pGEM-T vector and sequenced. After partial sequencing of the D4-GDI intron (data not shown), PCR products were analyzed by direct sequencing methods using the fluorescent forward primer (5′-CACCCAC TATACACATGTCTCT-3′) for the D4-GDI gene intron. Reh cells were also obtained from other laboratories and the D4-GDI gene was sequenced by the following method in order to eliminate any contamination of cells and to confirm the mutations. RT-PCR was performed with another N-terminal primer (5′-ACAGA GACGTGAAGCACTGAA-3′) and C-terminal primer (5′-GATG CATCAA TAAGGAAATGT-3′). These primers flanked the initial primers and were used to exclude contamination of PCR products and plasmids. PCR products were analyzed by direct sequencing method.

Construction of mt and wild-type D4-GDI expression vectors and short hairpin RNA vector for knockdown of Rho-GDI–α

Mutated D4-GDI cDNA of Reh cells was generated by RT-PCR. Wild-type (wt) D4-GDI cDNA was generated from HPB-ALL cells by RT-PCR. Vectors containing wt or mt D4-GDI cDNA with a myc-tag driven by the SRα promoter were constructed. This vector contained the neomycin-resistance (neo^r) gene driven by the SV40 promoter. The specific sequences for Rho-GDI small interfering RNA were searched by siDirect online software (RNAi Corporation, Tokyo, Japan). As a result, nucleotide number of human Rho-GDI–α 1191–1213 (3′UTR TCGGTCCCGTCTAAC CATGATGC) as Rho-GDI–α and scramble 23-nucleotide as control were generated. DNA-based small interfering RNA vectors were constructed in pBLOCK-iT6 DEST vector (Invitrogen, Carlsbad, CA, USA) for short hairpin RNA (shRNA) synthesis.

Transfection of wt or mt D4-GDI gene and shRNA vector for Rho-GDI knockdown into Raji cells

Wild-type or mt D4-GDI expression vector or shRNA vector for Rho-GDI knockdown was transfected into Raji cells by electroporation using a Gene Pulser (Bio-Rad, Hercules, CA, USA). The SRα–myc-tag vector or shRNA vector with scramble 23-nucleotide was transfected into Raji cells as a control. The Raji cells were cultured in culture media with G418 (800 μg/mL; Sigma-Aldrich, Tokyo, Japan) or blasticidin (10 μg/mL; Invitrogen, Carlsbad, CA, USA) for 14 days, followed by subcloning in a 96-well plate twice. Expression of D4-GDI or Rho-GDI–α protein was confirmed by Western blotting using a rabbit anti–D4-GDI or Rho-GDI polyclonal antibody (Zymed Laboratory, San Francisco, CA, USA). Blotted membranes were treated with peroxidase-conjugated anti-rabbit immunoglobulin antibody and visualized with electrochemiluminescence (Amersham-Pharmacia Biotech). The protein concentration was measured by BCA protein assay reagent (Pierce, Rockford, IL, USA).

Transplantation of leukemic cells into SCID mice

SCID mice (C.B.17 SCID mice, female, 7 to 9 weeks after birth; Clea, Tokyo, Japan) were maintained under specific pathogen-free conditions, and 2×10^7 Raji cells with/without wt or mt D4-GDI or Rho-GDI shRNA were suspended in 100 μL culture medium and injected into the tail veins of mice.

Analysis of leukemic cell invasion in SCID mice

Development of hemiparalysis in the mice was defined as the state in which they showed no motion of their hemilateral lower extremities. On day 17 or 20, when all mice were still alive and some showed hemiparalysis, the mice were sacrificed. Peripheral blood was prepared from the orbital vein plexus and cells were taken from the bilateral femurs and tibiae, and the spleen. The peripheral blood was subjected to hemolysis before being washed in phosphate-buffered saline (pH 7.4). Samples were then subjected to staining with anti-human CD19 monoclonal antibody (phycoerythrin-conjugated; DAKO, Glostrup, Denmark, diluted 1:100) for analysis with a flow cytometer (EPICS XL-MCL; Beckman Coulter, Hialeah, FL, USA). The systemic organs of mice were also prepared for pathological analysis by fixation in 10% formaldehyde in phosphate-buffered saline, embedding in paraffin, sectioned and then stained with hematoxylin-eosin. Immunohistochemical analyses were performed with anti-human CD19 monoclonal antibody and anti-proliferating cell nuclear antigen (PCNA) monoclonal antibody (Oncogene Science, Uniondale, NY, USA, diluted 1:50).

In vitro and in vivo proliferation assay

Proliferation rates of Raji cells with mt or wt D4-GDI or myc-tag only and shRNA vector for Rho-GDI knockdown or scramble 23-nucleotide were determined using the MTT method. These three clones were placed in eight wells of a round-bottomed 96-well plate at a concentration of 2×10^3 cells/100 μΛ/well and cultured for 48 hours, followed by addition of 5 mg/mL MTT (3-[4,5-dimethylthiazol-2-yl]-2,5-diphenyltetrazolium bromide; Sigma-Aldrich) at a concentration of 10 μL/well and further cultured for 4 hours. After the cells had settled on the plate, 100 μL 0.04 N HCl plus isopropanol was added. The resultant mixture was stirred and then measured using an enzyme-linked immunosorbent assay reader (Microplate Reader Model 450; Bio-Rad) for absorbance at 570 nm and 630 nm.

The in vivo proliferative capabilities of leukemic cells were investigated by the PCNA labeling index in situ [33]. The number of nuclear PCNA-positive cells and total cells in the vertebrae were counted in 10 fields.

Cell motility assay

Cell migration ability was assessed in 48-well chambers using polyvinylpyrrolidone-free polycarbonate membranes with 5-μm or 3-μm pores (NeuroProbe, Inc., Gaithersburg, MD, USA). RPMI-1640 supplemented with 1% pasteurized human plasma was placed in lower wells, and used to dilute the cells in upper wells. After 3 hours at 37°C, the membrane was removed, washed on the upper side with phosphate-buffered saline, then fixed and stained with DiffQuik (NeuroProbe). All assays were done in triplicate, and migrated cells were counted in five randomly selected

fields at 600-fold magnification. General and spontaneous migration was determined in the absence of chemokines.

Adhesion assays

Adhesion of Raji cells to the extracellular matrix or cells was assessed. Extracellular matrices (Matrigel; Becton-Dickinson, Mountain View, CA, USA), human fibronectin, laminin, and collagen type IV (Asahi Techno Glass, Funabashi, Chiba, Japan) were used in the 24-well Biocoat cellware (Becton-Dickinson). Human bone marrow stromal cells, which were obtained from bone marrow specimens of nonhematological patients, with informed consent, were seeded in 24-well plates prior to 24-hour adhesion assays. Cells were fluorescently labeled with 2 μM 2,7-bis-(2-carboxyethyl)-5 (and 6) carboxyfluorescein (BCECF; Molecular Probes, Eugene, OR, USA) for 30 minutes at 37°C. Labeled cells were washed twice, resuspended with RPMI to achieve a concentration of 2×10^5 cells/mL, and added to each well. After incubation with fixative, plates were washed and the number of fluorescent cells bound was determined by proportionality to the remaining BCECF fluorescence measured using a FluorImager 595 (Molecular Dynamics).

Affinity-precipitation of cellular GTP-bound Rho, Cdc42, and Rac

Ren et al. [34] developed a method based on evidence that Rho effectors interact only with GTP-bound Rho for the measurement of Rho activity [34]. Binding of Rho to the Rho-binding domain (RBD) from the effector protein Rhotekin inhibited both the intrinsic and GAP-enhanced GTPase activity of Rho [35]. Therefore, Rhotekin RBD was used to affinity-precipitate cellular GTP-Rho. Cells were washed with ice-cold Tris-buffered saline and lysed in RIPA buffer (50 mM Tris [pH 7.2], 1% Triton X-100, 0.5% sodium deoxycholate, 0.1% sodium dodecyl sulfate, 500 mM NaCl, 10 mM $MgCl_2$, 10 mg/mL each of leupeptin and aprotinin, and 1 mM phenylmethylsulfonyl fluoride). Cell lysates were clarified by centrifugation at 13,000*g* at 4°C for 10 minutes, and equal volumes of lysates were incubated with GST-RBD (a fusion of RBD with glutathione S-transferase, 20 μg) beads at 4°C for 45 minutes. Beads were washed four times with buffer B (Tris buffer containing 1% Triton X-100, 150 mM NaCl, 10 mM $MgCl_2$, 10 mg/mL each of leupeptin and aprotinin, and 0.1 mM phenylmethylsulfonyl fluoride). Bound Rho proteins were detected by Western blotting using an anti-RhoA monoclonal antibody (Santa Cruz Biotechnology, Santa Cruz, CA, USA). Densitometric analysis was performed using NIH image version 1.62. The amount of RBD-bound Rho was normalized to the total amount of Rho in cell lysates for the comparison of Rho activity (level of GTP-bound Rho) in different samples. Depending on cell conditions and types, and different batches of GST-RBD, the RBD-bound Rho accounts for ~0.5% to 5% of total Rho. The measurement of Rac activity was performed using the Rac Activation Assay kit (Cytoskeleton, Denver, CO, USA) according to the manufacturer's protocol.

[^{3}H]GDP dissociation assay

D4-GDI (wt, V68L, V69A, and both V68L and V69A mutations) protein was synthesized using Baculo-viral expression system with Bac-to-Bac HT vector (Invitrogen, Carlsbad, CA, USA) and Sf9 cells. His-tag D4-GDI proteins in cell lysates were purified using Ni-NTA agarose and ProBond Purification system (Invitrogen) according to the manufacturer's protocol. The inhibitory activities of wt, mt (V68L, V69A, and both V68L and V69A mutations), and wt plus each mt D4-GDI on GDP dissociation from isoprenylated Rho were determined using a filtration assay, as described previously by Chuang et al. [13]

Statistical analysis

All results were evaluated using Student's *t*-test–based statistics. Experiments were performed at least three times each.

Results

Detection of mutations of D4-GDI cDNA or genomic DNA in human leukemic cells

Results of DNA sequence analysis of the D4-GDI cDNA from the human leukemic cell lines are shown in Figure 1. Two point mutations at positions 276 (a G to C change) and 280 (T to C) were found in the D4-GDI cDNA of the Reh cell line. No mutations of the D4-GDI gene were detected in the D4-GDI genes of HPB-ALL, Raji, Ramos, and Daudi cell lines or in normal human peripheral blood lymphocytes (data not shown). Direct sequencing analysis of genomic DNA showed that these mutations were present on one allele (Fig. 2). These two point mutations of D4-GDI in the Reh cell led to conversions of valine 68 to leucine and valine 69 to alanine. The alignment of the predicted amino acid sequences of mt D4-GDI, wt D4-GDI, and other Rho-GDI family genes are shown in Figure 1. These two mutations exist in the partially conserved region at the amino acid level.

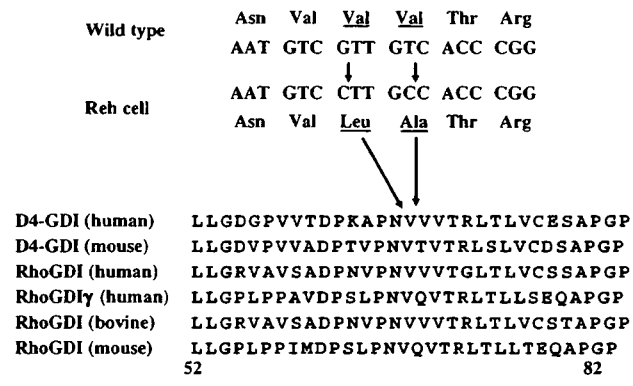

Figure 1. Two point mutations of D4-GDI cDNA in Reh cells and alignment of the predicted amino acid sequence. Two point mutations in D4-GDI were detected in Reh cells (arrows). These changes resulted in a guanine to cytosine substitution at position 276 and a thymine to cytosine substitution at nucleotide 280 (underlined). The alignment of predicted amino acid sequences of D4-GDI and Rho-GDI family genes. The two D4-GDI point mutations in Reh cells led to a valine 68 to leucine change and a valine 69 to alanine change. This region is highly conserved in Rho-GDI family members.

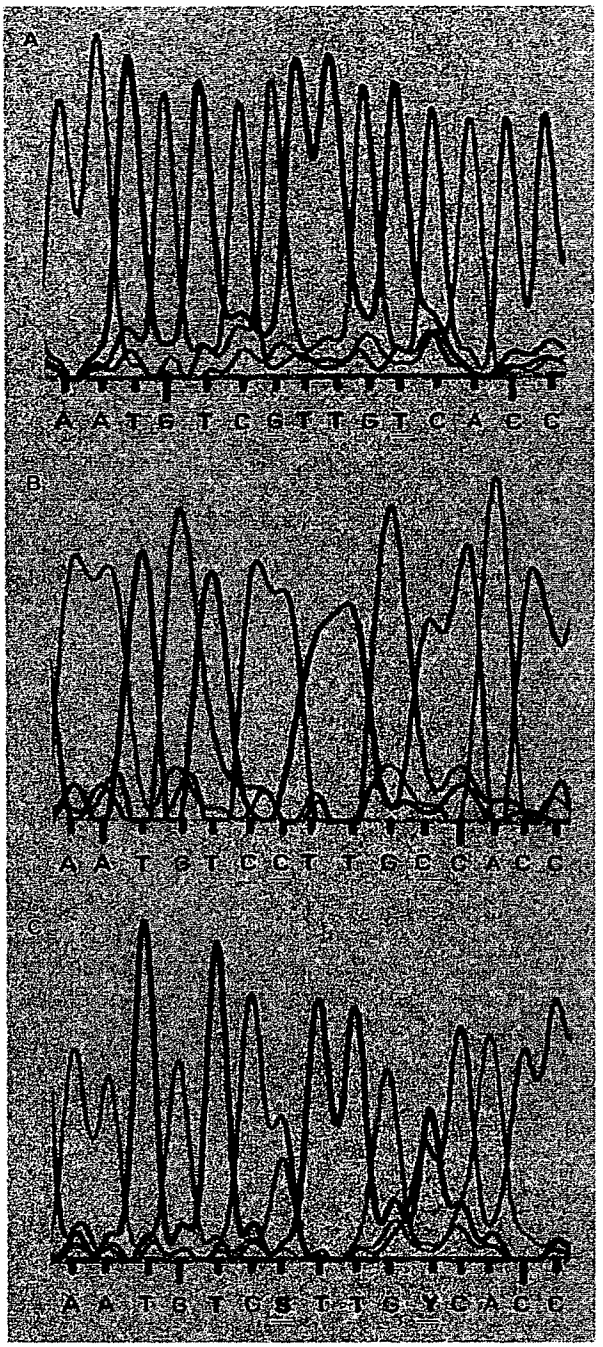

Figure 2. Heterozygous mutations of the D4-GDI gene in Reh cells. (**A**) Normal D4-GDI sequence from normal human peripheral blood lymphocytes. (**B**) Two point mutations in D4-GDI in Reh cells (underlined). These changes resulted in a guanine to cytosine substitution at position 276 and a thymine to cytosine substitution at nucleotide 280. (C) Direct sequence analysis of DNA amplified from genomic DNA of Reh cells showed identical mutations in one allele (heterozygous). Arrowheads indicate the two peaks, guanine and cytosine at position 276, and thymine and cytosine at nucleotide 280.

Gene transfer of wt or mt D4-GDI expression vector into Raji cells

A human leukemic cell line (Raji) was used in order to clarify the functions of mt or wt D4-GDI, because there were no mutations of D4-GDI gene in the Raji cells. Some clones with wt D4-GDI, mt D4-GDI, or the myc-tag vector were obtained and used in subsequent experiments. Expression of exogenous D4-GDI in these clones was confirmed by Western blotting using anti–D4-GDI polyclonal antibody. These cells expressed a protein of approximately 29 kDa, which was recognized by the D4-GDI antibody (Fig. 3A). The lower bands were endogenous D4-GDI in Raji cells and the upper bands were the exogenous D4-GDI with the myc-tag. We detected the expression of exogenous D4-GDI protein by Western blotting using anti-myc-tag antibody (9E10) (data not shown). The amounts of exogenous D4-GDI were almost the same as the endogenous D4-GDI in clones 21 and 26 with wt D4-GDI and in clone 13 with mt D4-GDI.

Gene transfer of a shRNA vector for Rho-GDI knockdown into Raji cell clones with wt or mt D4-GDI expression vector

The Raji cells with the wt D4-GDI (clone 3) or the mt D4-GDI (clone 13) were transferred with a shRNA vector for Rho-GDI knockdown or a vector of scramble shRNA as a control. Clones that were selected by blasticidin were examined by Western blotting using anti–Rho-GDI polyclonal antibody. Expression of Rho-GDI in clone wt3-21 and mt13-27 with Rho-GDI shRNA vector was decreased compared with clone wt3-1 and mt13-3 with scramble shRNA vector as a control (Fig. 3B). The clones with decreased expression under a quarter of Rho-GDI were established from the Raji cells with the wt D4-GDI, on the other hand, clones with a decreased expression under a half of Rho-GDI were not obtained from the Raji cells with the mt D4-GDI.

Exogenous D4-GDI expressions alter invasion of human leukemic cells in SCID mice

Wild-type D4-GDI clones (21 and 26), mt D4-GDI clones (13 and 20), and two myc-tag clones (1 and 4) were inoculated into SCID mice intravenously. The hemiparalysis and survival curves are summarized in Figure 4A. All mice (n = 18) inoculated with the myc-tag clone (as a control) developed hemiparalysis at 18 to 41 days (mean: 24 days) after transplantation. Histological analysis of systemic organs on day 20 revealed that the myc-tag clones invaded the liver in two of the nine mice (22%). Myc-tag clones were present in peripheral blood (3–52% of white blood cells) and bone marrow (3–66% of mononuclear cells) on day 20. Myc-tag clones infiltrated both ovaries, as well. There were no invasions of myc-tag clones into the brain, salivary glands, lungs, kidneys, digestive tract, heart, adrenal glands, spleen, or thymus. In the mice with hemiparalysis, numerous monotonous blasts occupied the bone marrow of vertebrae and femora, and also extended beyond the bone into the epidural space of the spinal cord, and into neighboring muscles (Fig. 5A). The murine hematopoiesis in bone marrow was markedly suppressed

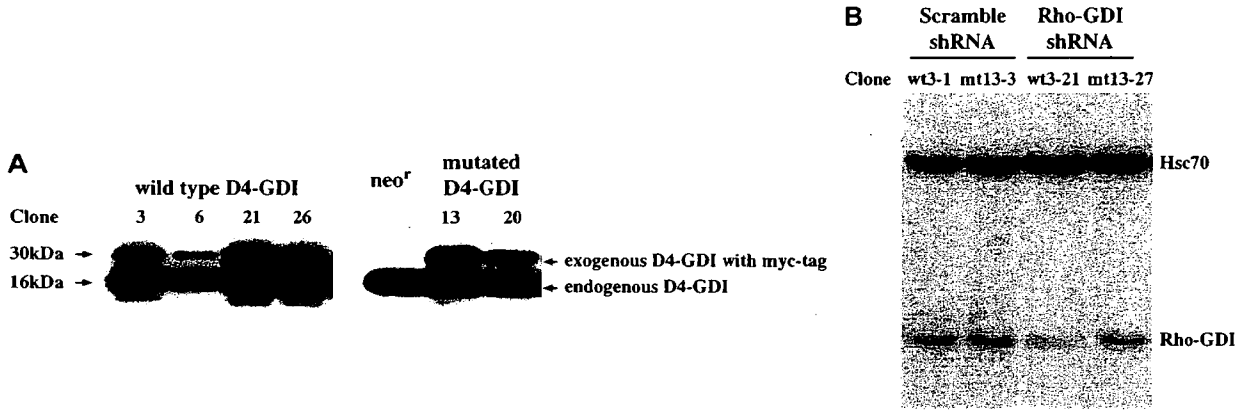

Figure 3. Gene transfer of wild-type or mutated D4-GDI expression vector into Raji cells and a vector of shRNA for Rho-GDI knockdown. (**A**) The Raji cells carrying the D4-GDI gene (clones 3, 6, 21, and 26 with wild-type D4-GDI vector and clone 13 and 20 with mutated D4-GDI vector) were prepared in Laemmeli's buffer and resolved by sodium dodecyl sulfate polyacrylamide gel electrophoresis. Western blotting was performed using anti-D4-GDI polyclonal antibody, peroxidase-conjugated secondary antibody, and electrochemiluminescence for visualization. The transfected cells expressed proteins of approximately 29 kDa and 30 kDa. The 29-kDa bands were endogenous D4-GDI and the upper bands were exogenous D4-GDI with myc tag. (**B**) The Raji cells with the wild-type (wt) D4-GDI (clone 3, wt3) or the mutated (mt) D4-GDI (clone 13, mt13) were transferred with a vector of shRNA for Rho-GDI knockdown. Selected clones were examined by Western blotting using anti-Rho-GDI polyclonal antibody. Expression of Rho-GDI in clone wt3-21 and mt13-27 with Rho-GDI shRNA vector was decreased compared with clone wt3-1 and mt13-3 with scramble shRNA vector as a control.

by infiltration of human leukemic cells. In addition, the spinal cord showed spongiosis, suggesting that development of hemiparalysis in these mice was attributable to invasion of the epidural space by leukemic cells (Fig. 5A). All mice inoculated with myc-tag clones died at 20 to 43 days posttransplantation.

Hemiparalysis in SCID mice inoculated with wt D4-GDI clones was apparently delayed as compared with the mice inoculated with myc-tag clones. These mice developed hemiparalysis (Fig. 4A). Eighteen of the 26 had hemiparalysis at 18 to 49 days (mean: 33.9 days, $p < 0.01$) after transplantation. Some of the SCID mice inoculated with wt D4-GDI clones developed hemiparalysis during the 60-day observation period (69% of all mice). The remaining mice survived more than 60 days (31% of all mice). There were no invasions of Raji cells with wt D4-GDI overexpression in the liver on day 20 after transplantation (0 of the 6 mice). The wt D4-GDI clones were present in peripheral blood (3–9% of white blood cells) and bone marrow (4–10% of white blood cells) on day 20.

On the other hand, SCID mice inoculated with mt D4-GDI clones began to develop hemiparalysis earlier, i.e., on day 14, after transplantation as compared with the mice inoculated with myc-tag clones, which developed similar paralysis after day 18 posttransplantation (Fig. 4A). All mice with mt D4-GDI ($n = 20$) developed hemiparalysis at 14 to 20 days (mean: 17.4 days, $p < 0.01$) after transplantation.

Histological analysis of mice inoculated with the mt D4-GDI clones revealed hepatic invasion of leukemic cells on day 17 in 8 of the 10 mice (80%), and all had larger invasive areas than the control myc-tag mice (Fig. 5B and C). Furthermore, invasions of Raji cells into the brain, kidneys, and ovaries in some of the mt D4-GDI clone–transplanted mice were found (date not shown). All mice died at 17 to 26 days posttransplantation.

The wt D4-GDI clones (wt3-1 or wt3-21) or mt D4-GDI clones (mt13-3 or mt3-27) with a vector for shRNA of Rho-GDI or a vector of scramble shRNA, respectively, were inoculated into SCID mice intravenously because the effect of mt D4-GDI in leukemic cell infiltration under the condition of decreased expression of Rho-GDI was examined. The hemiparalysis and survival curves are summarized in Figure 4B. The time course of development of hemiparalysis in SCID mice inoculated with wt3-1 clone was similar to mice inoculated with wt3-21 clone. Furthermore, hemiparalysis of mice inoculated with mt13-27 clone was not altered compared with the mice inoculated with mt13-3 clone as a control.

In vitro and in vivo cell proliferation

We examined whether the altered invasiveness of leukemic cells in vivo was attributable to certain changes in their proliferative abilities. However, MTT assay indicated that there were no differences in proliferation among wt D4-GDI clones, mt D4-GDI clones, and myc-tag clones in vitro (Fig. 6). An immunohistochemical analysis using anti-PCNA antibody was done in order to identify the proportion of in situ leukemic cells in S phase. PCNA is expressed in the nuclei of cells in the S phase in parallel with incorporation of bromodeoxyuridine or [^{3}H]-thymidine [1,33]. Almost all PCNA-positive cells in the bone marrow were human leukemic cells. There were no significant differences among the PCNA-labeling indices of wt D4-GDI clones, mt D4-GDI clones, and myc-tag clones (data not shown). These results indicate that neither wt nor mt D4-GDI expression altered leukemic cell invasion via induction of cell proliferation. The proliferating activity of the wt

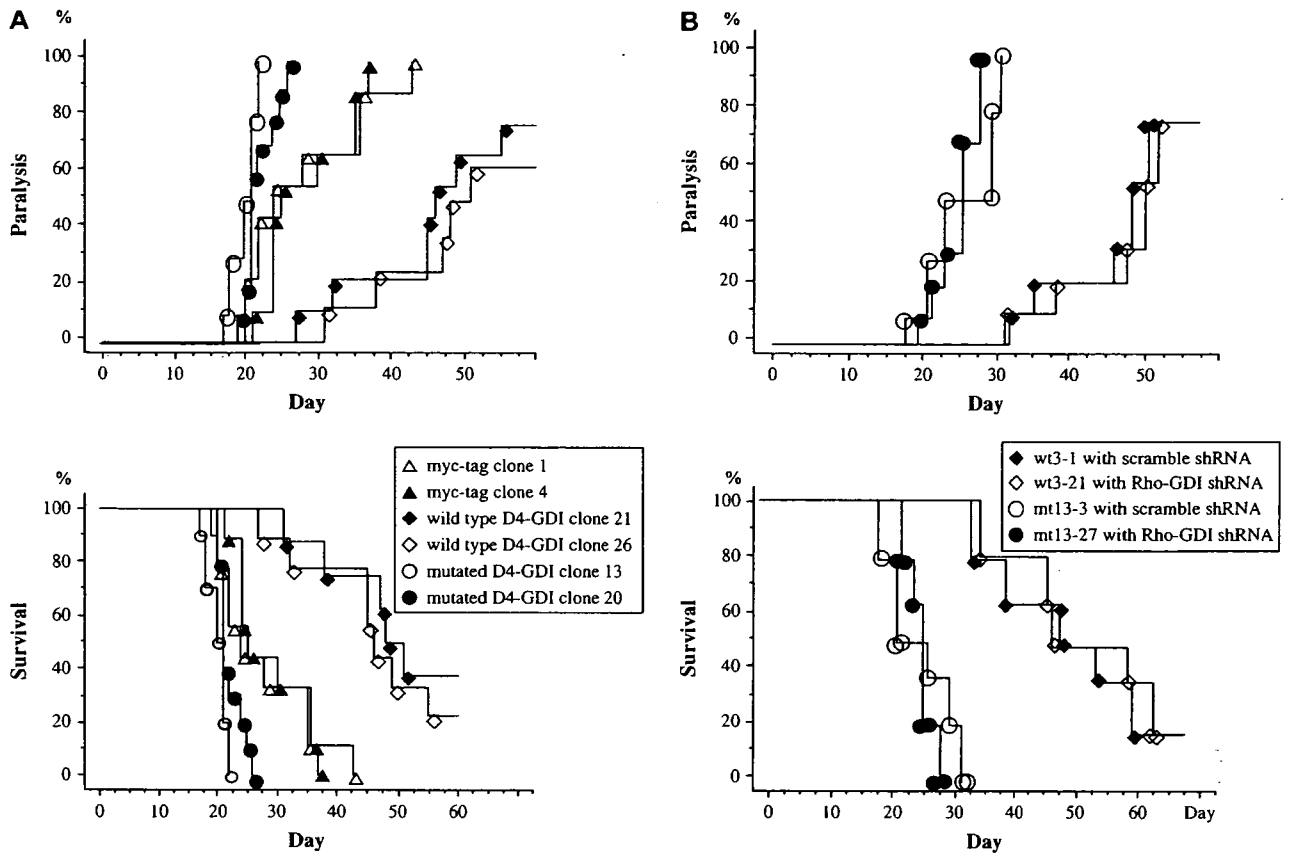

Figure 4. Alteration of hemiparalysis and survival with exogenous D4-GDI expressions in leukemic cells. (**A**) Hemiparalysis was observed in severe combined immune deficient (SCID) mice inoculated with wild-type D4-GDI clones (21 and 26), mutated D4-GDI clones (13 and 20) and myc-tag clones (1 and 4). The mice inoculated with wild-type D4-GDI clones developed hemiparalysis later than myc-tag clone–transplanted mice. On the other hand, the mutated D4-GDI clone–transplanted mice developed hemiparalysis earlier than the myc-tag clone–transplanted mice. Data on the appearance of hemiparalysis; Myc-tag clone transplanted mice (n = 18) at 18 to 41 days (mean: 24 days), wild-type D4-GDI–transplanted mice (n = 26) at 18 to 49 days (mean: 33.9 days, $p < 0.01$), and mutated D4-GDI–transplanted mice (n = 20) at 14 to 20 days (mean: 17.4 days, $p < 0.01$) after transplantation. (**B**) The wild-type D4-GDI clones (wt3-1 or wt3-21) or mutated D4-GDI clones (mt13-3 or mt3-27) with a vector for shRNA of Rho-GDI or a vector of scramble shRNA were inoculated into SCID mice. The hemiparalysis and survival curves are not altered. The time course of development of hemiparalysis in SCID mice inoculated with wt3-1 clone was similar to mice inoculated with wt3-21 clone. The hemiparalysis of mice inoculated with mt13-27 clone was not altered compared with the mice inoculated with mt13-3 clone as a control.

D4-GDI clones (wt3-1 or wt3-21) or mt D4-GDI clones (mt13-3 or mt3-27) with a vector for shRNA of Rho-GDI or a vector of scramble shRNA were examined using MTT assay in order to observe the function of mt D4-GDI under the condition of decreased expression of Rho-GDI. As a result, no differences between these clones (wt3-1, wt3-21, mt13-3 or mt3-27) were revealed (data not shown).

Alteration of cellular motile activity by exogenous D4-GDI expression

We attempted to estimate changes in general cell motility in response to exogenous D4-GDI expression in leukemic cells, because we did not detect differences in cell proliferation of wt or mt D4-GDI clones in vitro or in vivo. As a result, mt D4-GDI clones had increased cell motilities ($p < 0.001$), and wt D4-GDI clones had decreased cell motilities ($p < 0.01$) as compared with the myc-tag clones, without chemokines in vitro (Fig. 7). The cellular motile activities of each clone would correspond to the invasive activities (see Figs. 4 and 5). Mutated D4-GDI clone 13 showed the highest motile activity in vitro and the highest invasive activity in vivo. The motile activity of wt or mt D4-GDI clones (wt3-1, wt3-21, mt13-3, or mt3-27) with a vector of scramble shRNA or a vector for shRNA of Rho-GDI were examined in order to analyze the function of mt D4-GDI under the condition of decreased expression of Rho-GDI. As a result, no alterations between clone wt3-1 and wt3-21, or between clone mt13-3 and mt3-27, were observed (data not shown).

Augmentation of cell adhesion by mt D4-GDI expression

Cell motility consists of multiple and complex steps, including a response against chemotactic factors, cytoskeletal organization, and cell adhesion. We investigated whether exogenous D4-GDI expression altered the motile activity of leukemic cells through changes in cell adhesion. Adhesion of Raji cells, which contain mt or wt D4-GDI or the

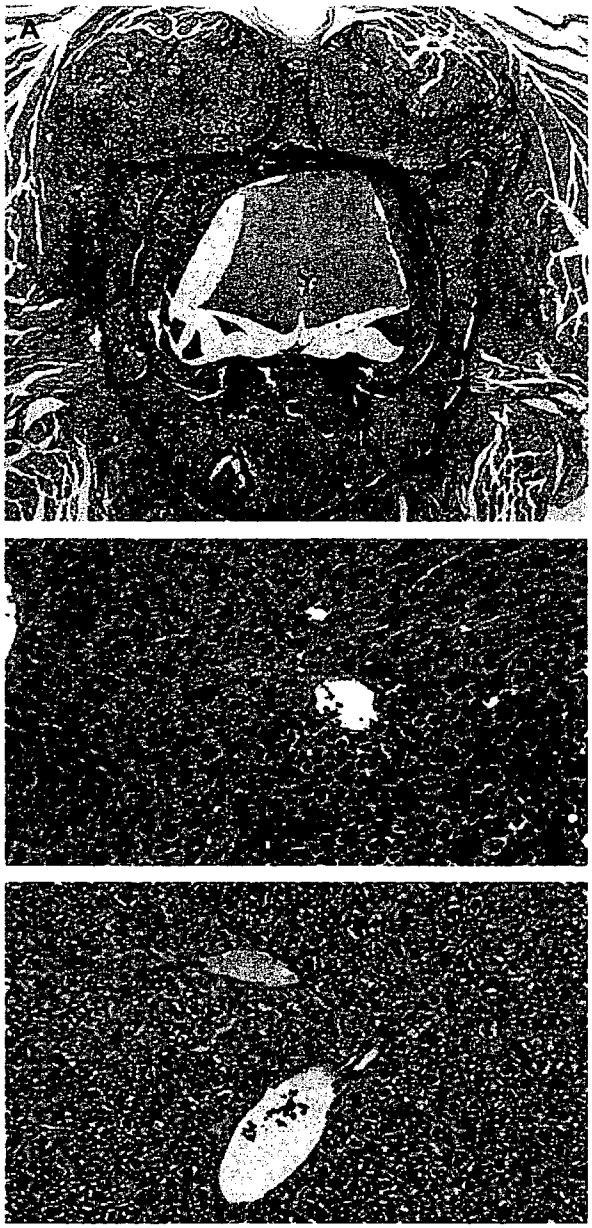

Figure 5. Raji cell invasion in severe combined immune deficient (SCID) mice. (**A**) The vertebra of an SCID mouse inoculated with myc-tag clone 1 is shown in a transverse section (hematoxylin-eosin staining). Raji cells have invaded the bone marrow, surrounding tissues, and the epidural space (day 17 after transplantation). The result is spongiosis, due to compression myelopathy of the spinal cord. S and L indicate the spinal cord and human leukemic (Raji) cells, respectively. Original magnification ×100. (**B**) Hepatic invasion by mutated D4-GDI clone 13 is shown. Original magnification ×120. (**C**) On other hand, there was no hepatic invasion in mice inoculated with wild-type D4-GDI clone 26. Original magnification ×120.

myc-tag only, to the extracellular matrix or cells was assessed as described previously [1]. Extracellular matrices (Matrigel [Becton-Dickinson], human fibronectin, laminin, and collagen type IV) were placed in 24-well dishes. In order to quantitate cell-adhesion activity, the leukemic cells were labeled with 2 μM BCECF, washed, and the fluorescence was then measured with a FluorImager 595. As a result, no significant differences in adhesiveness between these clones on each extracellular matrix (Matrigel, human fibronectin, laminin, and collagen type IV) were observed (data not shown). However, differences in adhesiveness to the stromal cells were obvious. In contrast to the myc-tag and wt D4-GDI clones, the mt D4-GDI clones showed augmented adhesiveness to human bone marrow stromal cells ($p < 0.05$) (Fig. 8). There was a significant difference in adhesion to human stromal cells between the myc-tag clones and the wt D4-GDI clones.

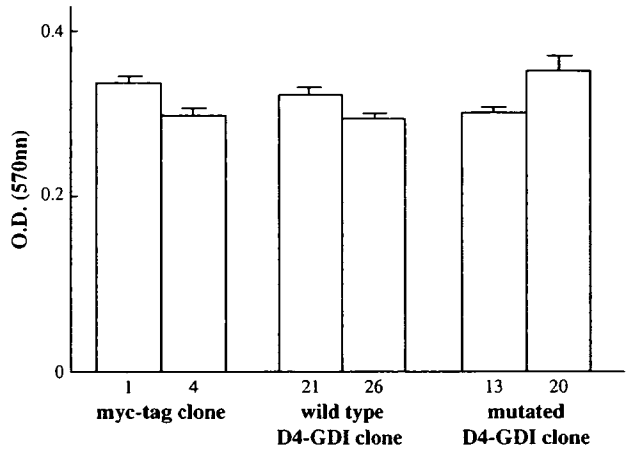

Figure 6. Exogenous D4-GDI expression does not change cell growth rates. The in vitro growth rates of myc-tag clones, wild-type D4-GDI clones, and mutated D4-GDI clones were compared by performing MTT assays. There were no significant differences in proliferative ability among these clones.

Cell-adhesion activity of wt or mt D4-GDI clones (wt3-1, wt3-21, mt13-3, or mt3-27) with a vector of scramble shRNA or a vector for shRNA of Rho-GDI was examined in order to analyze the function of mt D4-GDI under the condition of decreased expression of Rho-GDI. As a result, no differences in adhesion activity between clone wt3-1 and wt3-21, or between clone mt13-3 and mt3-27, were revealed (data not shown).

Detection of cellular GTP-bound Rho, Cdc42, and Rac in leukemic cells

We investigated whether D4-GDI (wt or mt) overexpression in leukemic cells altered Rho and Rac activity. We employed a pull-down assay using RBD affinity-precipitation and Western blotting with anti-RhoA antibody (see Materials and Methods). The proportions of activated Rho (GTP-bound Rho/total Rho) did not differ among myc-tag, wt D4-GDI, and mt D4-GDI clones (Fig. 9). GTP-bound Rho accounted for 1.3% to 1.6 % of total Rho in all experiments. In order to confirm the absence of differences in Rho activity among these clones, the immunoprecipitation with anti-RhoA antibody was carried out after metabolic pulse chase labeling with [^{35}S]-GTPγs. The uptakes of [^{35}S]-GTPγs into RhoA for 8 hours in myc-tag, wt D4-GDI, and mt D4-GDI clones were not different (data not shown). Furthermore, no differences of the

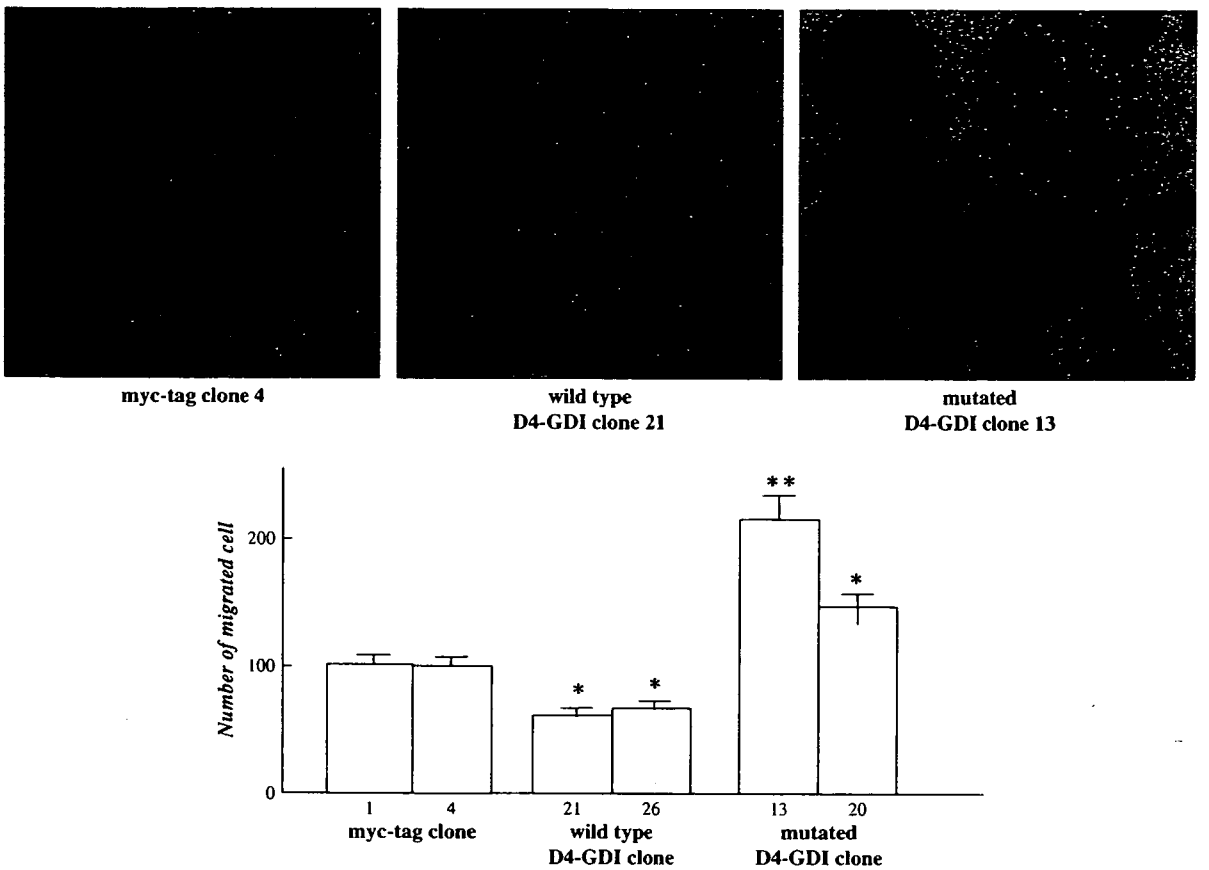

Figure 7. Alteration of cell motility by wild-type or mutated D4-GDI overexpression. The in vitro cellular motile activities of myc-tag clones, wild-type D4-GDI clones, and mutated D4-GDI clones were compared using a chemotaxis chamber (NueroProbe), without hemotactic factors (see Materials and Methods). In contrast to myc-tag clones 1 and 4, mutated D4-GDI clones 13 and 20 showed markedly increased motilities. On the other hand, wild-type D4-GDI clones 21 and 26 showed significantly decreased cell motilities. The upper colored figures show results representative of migrated leukemic cells stained with Diff-Quik (NeuroProbe). Data are represented as mean values. Error bars show standard error of mean. ** and * indicate statistically significant increases ($p < 0.001$ and $p < 0.01$, respectively) as compared to data from myc-tag clone 1 or 4.

Cdc42 and Rac activities between these clones were also observed (Fig. 9A).

Alterations of cellular GTP bound-Rho under the condition of decreased expression of Rho-GDI in leukemic cells with wt D4-GDI or mt D4-GDI overexpression were examined. The pull-down assay for Rho using the wt or mt D4-GDI clones (wt3-1, wt3-21, mt13-3, or mt3-27) with a vector of scramble shRNA or a vector for shRNA of Rho-GDI were done. As a result, the GTP-bound Rho in Rho-GDI knockdown clones (both wt3-21 and mt13-27) was slightly increased compared with clones with scramble shRNA vector (wt3-1 and mt13-3). Especially the difference of GTP-bound Rho/total Rho ratio between mt13-3 and mt13-27 was greater than the difference between wt3-1 and wt3-21. This dissimilarity between wt D4 clones and mt D4 clones in Rho activation by Rho-GDI knockdown may show that the mt D4-GDI proteins impair certain D4-GDI functions.

These results show the exogenous mt D4-GDI expression to be involved in the invasiveness of human leukemic cells through augmentation of cell motility and/or cell-adhesion activity. The altered phenotypes of leukemic cells may be caused by Rho activation due to the mt D4-GDI expression.

Mutated D4-GDI functioned in a dominant negative manner in the inhibition of GDP dissociation from Rho in vitro

While human D4-GDI has been previously shown to inhibit GDP dissociation from Rho family GTPases, we used purified recombinant proteins of wt and mt D4-GDI (V68L or V69A or both V68L and V69A) to directly compare their activities. Sf9 cell–expressed isoprenylated Rho were preloaded with [^{3}H]GDP, and the ability of wt D4-GDI, mt D4-GDIs, and wt plus mt D4-GDIs to inhibit dissociation of the nucleotide was determined. The dissociation of [^{3}H]GDP from Rho was totally blocked by wt D4-GDI (Fig. 10). The dissociation activity of [^{3}H]GDP from Rho by mt D4-GDI with both mutations of V68L and V69A was significantly low. On the other hand, the dissociation activity of mt D4-GDI with single mutation (V68L or V69A) was mild. Furthermore, inhibition of dissociation of [^{3}H]GDP

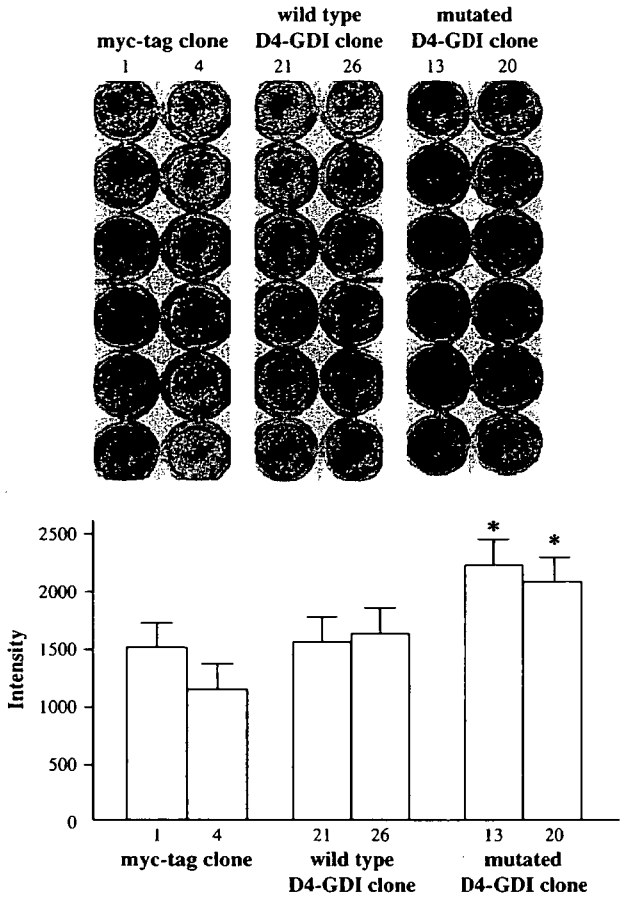

Figure 8. Augmentation of cell adhesion to human bone marrow stromal cells by mutated D4-GDI expression. The cell-adhesion activities of myc-tag clones, wild-type D4-GDI clones, and mutated D4-GDI clones were compared by using quantitative adhesion assays with fluorescent labeling of living cells (see Materials and Methods). In the upper panel, the unlabeled human stromal cells (invisible) attached to all wells and 2,7-bis-(2-carboxyethyl)-5 (and 6) carboxyfluorescein–labeled Raji cell clones, which adhered to the stromal cells were visible like black granules. The vertical line (six wells) represents data derived from one clone. In contrast to myc-tag clones 1 and 4, the mutated D4-GDI clones showed increased adhesiveness to human bone marrow stromal cells ($p < 0.05$). There was no significant difference in adhesion to human stromal cells between the myc-tag clones and wild-type D4-GDI clones. Data are represented as mean values. Error bars show standard error of mean. *Indicates a statistically significant increase ($p < 0.05$) as compared to data from myc-tag clone 1 or 4.

from Rho by wt D4-GDI was impaired by the addition of mt D4-GDI with both mutations of V68L and V69A. The negative effect by the addition of mt D4-GDI with single mutation of V68L orV69A to wt D4-GDI was not observed. As a result, the mt D4-GDI proteins with two mutations may function in a dominant negative manner in vitro.

Discussion

We identified two point mutations of D4-GDI in the human B-cell leukemic cell line. The region of D4-GDI containing these point mutations, which result in amino acid substitutions, is partially conserved in Rho-GDI family genes (Fig. 1). X-ray analysis of the three-dimensional structure of Rho-GDI suggested that these mutations of D4-GDI are in a β-sheet structure [36]. This region is at the back of the continuous surface adjacent to the isoprene-binding site of Rho-GDI, and could easily contact the bound GTPase and impart GDI activity. Robson protein secondary structure prediction suggested that these mutations may influence the β-sheet region [37]. The dissociation activity of GDP of D4-GDI with both mutations of V68L and V69A was decreased greater than the dissociation activity of mt D4-GDI with single mutation (V68L or V69A). Furthermore, dissociation of GDP from Rho by wt D4-GDI was significantly impaired by the addition of mt D4-GDI with both mutations of V68L and V69A. This result suggests that the D4-GDI proteins with two mutations may function in a dominant negative manner.

Thus, we speculated that this mt D4-GDI plays a role in development of hematological malignancy, and analyzed functions of mt D4-GDI in human leukemic cell invasion in vivo using a transplantation model of human leukemic cells into SCID mice. The SCID mice inoculated with Reh cells developed paraplegia 21 days after inoculation and all had died by days 26 to 27. The Reh cells infiltrated into bone marrow and around the spinal cord, with no involvement into peripheral blood, the spleen, liver, thymus or lymph nodes [1]. We identified mutations in the D4-GDI gene from human leukemic cells and showed that overexpression of mt D4-GDI in Raji cells accelerates leukemic cell invasion. Furthermore, we showed that overexpression of wt D4-GDI in Raji cells suppresses invasiveness. Additionally, there were no differences in cell growth rates among these clones, despite the altered invasiveness. On the other hand, cellular motile activity in the mt D4-GDI clones was augmented as compared with the myc-tag clones, and the motile activity of wt D4-GDI clones was significantly decreased. In the cell-adhesion assay, the mt D4-GDI clones showed increased adhesiveness to human bone marrow stromal cells. These findings indicate that the mt D4-GDI functions as a dominant negative molecule against endogenous D4-GDI.

Direct involvement of the Rho family in oncogenesis was discussed in a report [24]. Some GDS with a dbl-homology domain responsible for stimulating nucleotide exchange activity have been reported as potent oncogenes capable of transforming NIH-3T3 cells into a malignant phenotype (e.g., Dbl, Vav, and Lbc) [7,22]. Tiam1 was identified as an invasion-related gene and promoted leukemia progression through activation of the Rac signaling pathway [24]. In contrast to the function of Tiam1 in leukemic cells, Tiam1 and Rac have an invasion-suppressor role in epithelial cells [38]. Rho may also be involved in the increased mobility seen in metastasis through its control of the assembly of focal adhesions [39]. A study suggested that Rho regulates cadherin-mediated adhesion in small

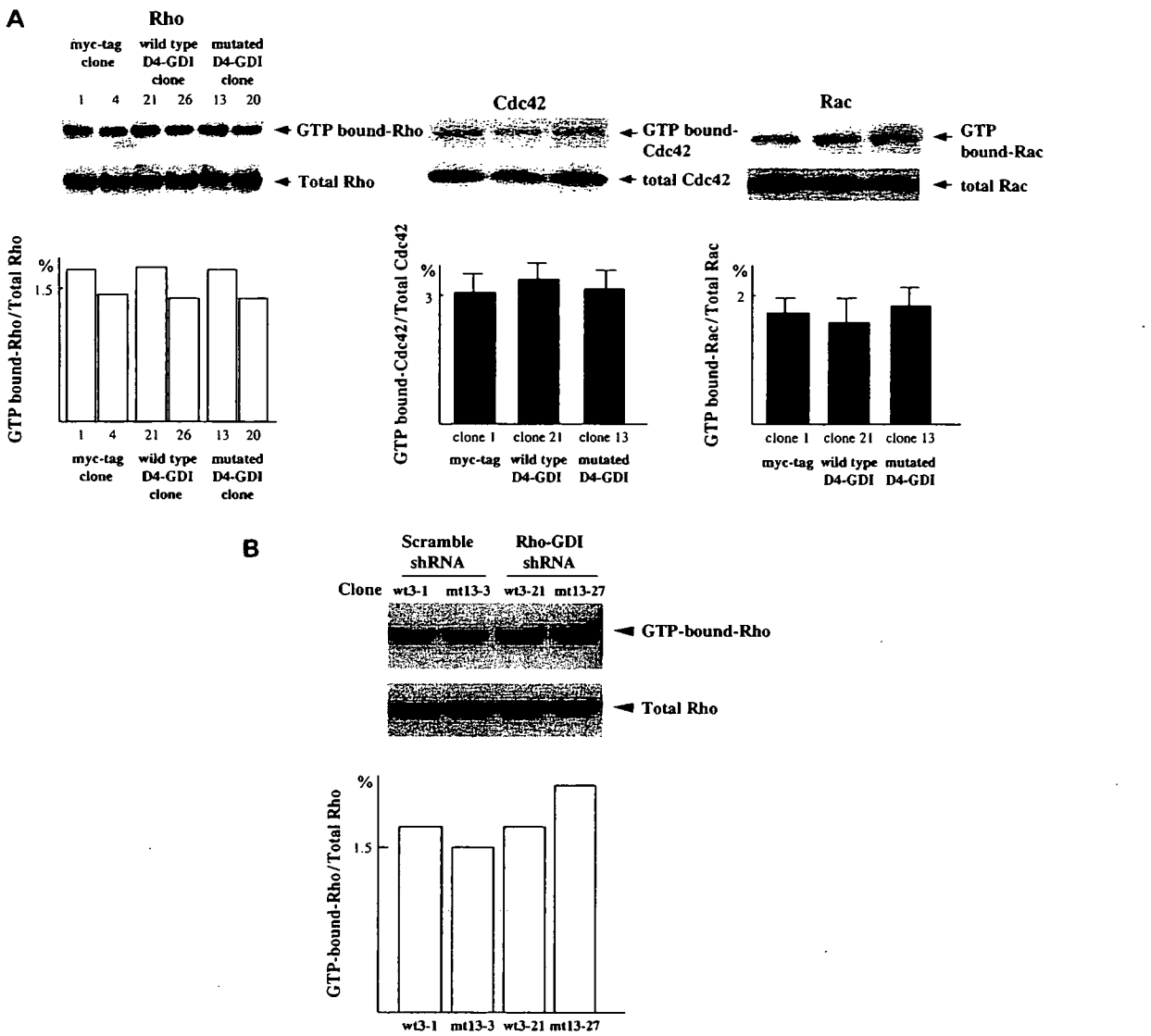

Figure 9. Detection of cellular guanine triphosphate (GTP)–bound Rho and Rac in leukemic cells. (**A**) Cells lysates were clarified by centrifugation, and equal volumes of lysates were incubated with 20 μg glutathione S-transferase (GST)–Rho-binding domain (RBD) beads. Beads were washed four times. Bound Rho proteins were detected by Western blotting using an anti-RhoA monoclonal antibody. The upper figures show the expressions of GTP-bound Rho and total Rho in all clones. The amounts of activated Rho (GTP-bound form) in all clones were almost the same. In order to quantitate the amount of GTP-bound Rho, a densitometric analysis was performed using NIH image version 1.62. The amount of RBD-bound Rho was normalized to the total amount of Rho in cell lysates for comparison of Rho activities (level of GTP-bound Rho) among different samples. The ratios of GTP-bound Rho to total Rho are shown in the lower graph. The GTP-bound Rho accounted for 1.3% to 1.6 % of total Rho in these six clones. There are no significant differences among the clones. The measurement of Rac activity was performed using the Rac Activation Assay kit (Cytoskeleton, Denver, CO, USA) according to the manufacturer's protocol. Amounts of activated Rac (GTP-bound form) in three clones were almost similar. In order to quantitate the amount of GTP-bound forms, a densitometric analysis was performed. The amount of GTP-bound Rac was normalized to the total amount of Rac in cell lysates for comparison of Rac activities among different samples. The ratios of GTP-bound Rac to total Rac are shown in the lower graph. The GTP- bound Rac accounted for 1.7% to 1.9% of total Rac in three clones, respectively. There are no significant differences among the clones. (**B**) Alterations of cellular GTP-bound Rho under the condition of decreased expression of Rho-GDI in leukemic cells with wt D4-GDI or mt D4-GDI overexpression. The pull-down assay for Rho using the wild-type or mutated D4-GDI clones (wt3-1, wt3-21, mt13-3, or mt3-27) with a vector of scramble shRNA or a vector for shRNA of Rho-GDI were done. As a result, the GTP-bound Rho in Rho-GDI knockdown mt D4 clones (mt13-27) was slightly increased compared with clones with scramble shRNA vector (wt3-1 and mt13-3) or Rho-GDI knockdown wt D4 clones (wt3-21).

cell lung carcinoma cells [40]. We reported that Rho activation augmented leukemic cell invasion through acceleration of cell adhesion, but not cell proliferation [1]. Itoh et al. [41] indicated rho-associated kinase played an essential part in tumor cell invasion, and that rho-associated kinase inhibitor may have potential as a therapy for prevention of malignant invasion and metastasis. In addition, Rho-GDI may also play a role in cancer invasion and metastasis

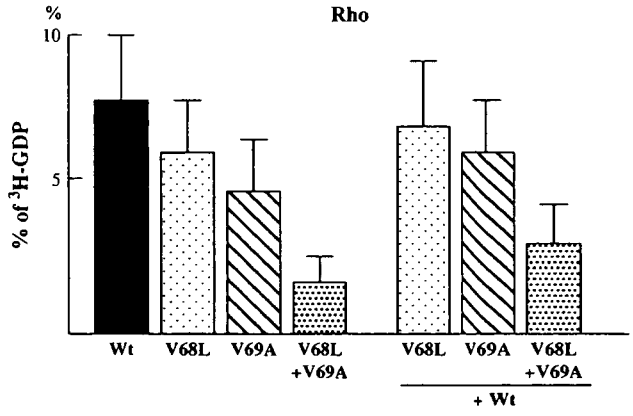

Figure 10. [^{3}H]GDP dissociation assay of Rho. The inhibitory activities of mutated (mt) D4 with two mutations of V68L and V69A on the dissociation of [^{3}H]GDP from isoprenylated Rho were less active than wild-type (wt) D4. The decreased dissociation activity of D4 with each single mutation (V68L orV69A) was slight. The results of the inhibitory activities of wt plus mt D4 with both mutations of V68L and V69A on the dissociation of [^{3}H]GDP from isoprenylated Rho showed mt D4 was dominant negative of wt D4 on the dissociation of [^{3}H]GDP from isoprenylated Rho. The dominant negative effect was not observed in the D4 with single mutation of V68L orV69A.

via involvement in the CD44 signaling pathway, because Rho-GDI coimmunoprecipitated with the CD44-ERM complex [42]. Recently, Zhang et al. reported that D4-GDI is expressed in a panel of breast cancer cell lines, but not in benign-derived mammary epithelial cells, and the D4-GDI modulates breast cancer cell–invasive activities [43]. These findings obviously indicate that the Rho family and its regulatory proteins play critical roles in the development and progression of malignancy.

Overexpression of wt D4-GDI or mt D4-GDI did not alter Rho or Rac activity, which was represented by the amount of GTP-bound Rho or Rac. D4-GDI functions both to inactivate Rho, via inhibition of the GDP dissociation from Rho, and to activate Rho, via suppression of the GTPase activity of Rho itself. Furthermore, D4-GDI has weaker GDP dissociation inhibitory activity (10-fold less) than Rho-GDI. Recently, Zhang et al. [43] reported that the activation status of Rac1, Cdc42, and RhoA was not altered as a result of D4-GDI depletion. In addition, like other Rho-GDIs, D4-GDI was postulated to bind and inhibit Rho GTPases. However, much yet remains to characterize the specificity of D4-GDI [15,16]. Although recombinant D4-GDI binds to purified Rac1, Cdc42, and RhoA, there is no evidence showing that they can form stable complexes in vivo [43]. Thus, the lack of changes in Rho or Rac activity in response to exogenous expression of wt D4-GDI or mt D4-GDI may be explained. On the other hand, the GTP-bound Rho in mt D4-GDI clone with Rho-GDI was slightly increased in contrast to mt D4-GDI clone without Rho-GDI knockdown or wt D4-GDI clones with/without Rho-GDI knockdown. These results suggest that the altered phenotypes of leukemic cells may be partially caused by Rho activation due to mt D4-GDI expression. However, the invasiveness, motility, and adhesion activity of mt D4-GDI clone with Rho-GDI knockdown was not changed in spite of the mild Rho activation in the mt D4 clone. Ishizaki et al. [44] recently report that combined disruption of both the Rho-GDI and D4-GDI genes in mice resulted in reduction of marginal zone B cells in the spleen, retention of mature T cells in the thymic medulla, and a marked increase in eosinophil numbers. Our results may be explained by the fact that the level of Rho-GDI knockdown was insufficient in contrast to the null mutation of Rho-GDI gene.

It was shown that D4-GDI is specifically cleaved at two positions (residues 18–19 and 54–55) by two different apoptosis proteases, caspase-3 and caspase-1, respectively [17,45]. These consensus cleavage sequences are not present in either Rho-GDI or Rho-GDIγ. A truncated D4-GDI cleaved by caspase-1 is unable to effectively bind and regulate Rho family members. D4-GDI is a target protein of caspase-3 in the process of anti–IgM-mediated or Fas-dependent apoptosis [17,46]. The positions of point mutations found in D4-GDI are residues 68 and 69. Therefore, the positions of these mutations are 13 and 49 amino acids from the cleavage sequence. No significant differences in the apoptosis induced by anti-cancer reagents, i.e., methotrexate, cyclohexamide, and vincristine, were seen in Raji cells transferred with mt D4-GDI transgene (data not shown).

It has been reported that Rho-GDI forms a complex with Rho A, CDC42, and Rac, while CDC42 and Rac was not found to interact with D4-GDI. Furthermore, stimulation with phorbol ester led to phosphorylation of D4-GDI in U937 cells [15]. Their results suggested that D4-GDI can regulate specific signal pathways in hematopoietic cells.

D4-GDI is a highly abundant cytoplasmic protein in lymphocytes, and has had a highly conserved primary amino acid sequence since the divergence of mammalian species. However, D4-GDI–deficient mice and in vitro embryonal stem cell differentiation analysis indicated D4-GDI expression is not essential for hematopoiesis and did not clarify its function in hematopoietic cells [47,48]. Our results indicate that D4-GDI overexpression in transformed cells changes cell motility, cell adhesion, and invasiveness in some organs. In normal lymphocytes, D4-GDI may have a subtle, yet crucial, function related to cell motility and adhesion.

Li et al. [49] reported that D4-GDI might be involved in the progression of human cutaneous T-cell lymphoma using a cDNA microarray in the clonally related T-cell lines derived from different stages of a progressive T-cell lymphoma involving skin. They found the D4-GDI gene to be one of the downregulated genes in cells from an advanced, clinically aggressive stage lymphoma, in contrast to cells from an earlier, clinically indolent stage of lymphoma. Expression of D4-GDI mRNA in cells derived from the aggressive stage lymphoma was shown to be markedly decreased as compared with cells derived from

the earlier-stage lymphoma. This result is compatible with our data, showing overexpression of wt D4-GDI to reduce the invasiveness of human leukemic cells. Thus, D4-GDI may assure the progression and invasion of human leukemia through its mutations and/or its downregulation.

Accumulating recent evidence shows that D4-GDI is expressed not only in hematopoietic tissues, but also in non-hematopoietic neoplasms. Results of cDNA microarray analyses revealed that D4-GDI is upregulated in ovarian [50], and downregulated in bladder, carcinomas [51]. On the other hand, Theodorescu et al. [52] found that D4-GDI protein expression in bladder tumors is reduced as a function of bladder tumor progression. This result has suggested that D4-GDI is a metastasis suppressor gene in models of bladder cancer. In contrast, the results of Zhang et al. [43] show that increased expression of D4-GDI promotes cell invasiveness in breast cancer cells. These results suggest that the D4-GDI may have certain roles in the progression of different types of cancer. Thus, it is reasonable to propose that D4-GDI may be involved more generally in the invasive phenotype of human cancer.

Acknowledgments

We thank Dr. Martin Alexander Schwartz (The Scripps Research Institute, La Jolla, C, USA) for generously providing a expression vector of GST-RBD. We thank Ms. Megumi Takamatsu, Mrs. Michiko Takahashi, and Dr. Yan Xiu, for cell culture and animal care, Mr. Hiroshi Suzuki for immunohistochemistry and Mr. Kohji Takeichi for technical photographic support.

This work was supported by Grants-in Aid for Pediatric Research (9C-5, 12C-1) from the Ministry of Health and Welfare, a research grant from the Ministry of Education in Japan (05404022, 07670258, 07770163, 1770124, 11670193, 10307004), National Grant-in-Aid for the Establishment of a High-Tech Research Center in a Private University, Sankyo Foundation of Life Science, Tsumura Foundation for Medical Research, Kawano Foundation for Children Cancer Research, and Keio Gijuku Academic Development Funds and a special grant-in-aid for innovative and collaborative research projects at Keio University.

References

1. Fukushima S, Yamada T, Hashiguchi A, Nakata Y, Hata J. Augmentation of human leukemia cell invasion by the activation of small GTP-binding protein Rho. Exp Hematol. 2000;28:391–400.
2. Hall A. Small GTP-binding proteins and the regulation of the actin cytoskeleton. Annu Rev Cell Biol. 1994;10:31–54.
3. Takai Y, Sasaki T, Tanaka K, Nakanishi H. Rho as a regulator of the cytoskeleton. Trends Biochem Sci. 1995;20:227–231.
4. Narumiya S. The small GTPase Rho: cellular functions and signal transduction. J Biochem. 1996;120:215–228.
5. Hall A. Rho GTPases and the actin cytoskeleton. Science. 1998;279: 509–514.
6. Vojtek AB, Cooper JA. Rho family members: activators of MAP kinase cascades. Cell. 1995;82:527–529.
7. Van Aelst L, D'Souza-Schorey C. Rho GTPases and signaling networks. Genes Dev. 1997;11:2295–2322.
8. Lelias JM, Adra CN, Wulf GM, et al. cDNA cloning of a human mRNA preferentially expressed in hematopoietic cells and with homology to a GDP-dissociation inhibitor for the rho GTP-binding proteins. Proc Natl Acad Sci U S A. 1993;90:1479–1483.
9. Scherle P, Behrens T, Staudt LM. Ly-GDI, a GDP-dissociation inhibitor of the RhoA GTP-binding protein, is expressed preferentially in lymphocytes. Proc Natl Acad Sci U S A. 1993;90:7568–7572.
10. Adra CN, Manor D, Ko JL, et al. Rho-GDIγ: a GDP-dissociation inhibitor for Rho proteins with preferential expression in brain and pancreas. Proc Natl Acad Sci U S A. 1997;94:4279–4284.
11. DerMardirossian C, Bokoch GM. GDIs: central regulatory molecules in Rho GTPase activation. Trends Cell Biol. 2005;15:356–363.
12. Hart MJ, Maru Y, Leonard D, Witte ON, Evans T, Cerione RA. A GDP dissociation inhibitor that serves as a GTPase inhibitor for the Ras-like protein CDC42Hs. Science. 1992;258:812–815.
13. Chuang TH, Xu X, Knaus UG, Hart MJ, Bokoch GM. GDP dissociation inhibitor prevents intrinsic and GTPase activating protein-stimulated GTP hydrolysis by the Rac GTP-binding protein. J Biol Chem. 1993;268:775–778.
14. Takahashi K, Sasaki T, Mammoto A, et al. Direct interaction of the Rho GDP dissociation inhibitor with ezrin/radixin/moesin initiates the activation of the Rho small G protein. J Biol Chem. 1997;272. 23371–22375.
15. Gorvel JP, Chang TC, Boretto J, et al. Differential properties of D4/LyGDI versus RhoGDI: phosphorylation and rho GTPase selectivity. FEBS Lett. 1998;422:269–273.
16. Golovanov AP, Chuang TH, DerMardirossian C, et al. Structure-activity relationships in flexible protein domains: regulation of rho GTPases by RhoGDI and D4 GDI. J Mol Biol. 2001;305:121–135.
17. Na S, Chuang TH, Cunningham A, et al. D4-GDI, a substrate of CPP32, is proteolyzed during Fas-induced apoptosis. J Biol Chem. 1996;271:11209–11213.
18. Krieser RJ, Eastman A. Cleavage and nuclear translocation of the caspase 3 substrate Rho GDP-dissociation inhibitor, D4-GDI, during apoptosis. Cell Death Differ. 1999;6:412–419.
19. Bos JL. Ras oncogenes in human cancer: a review. Cancer Res. 1989; 49:4682–4689.
20. Moscow JA, He R, Gnarra JR, et al. Examination of human tumors for rhoA mutations. Oncogene. 1994;9:189–194.
21. Boivin D, Bilodeau D, Beliveau R. Regulation of cytoskeletal functions by Rho small GTP-binding proteins in normal and cancer cells. Can J Physiol Pharmacol. 1996;74:801–810.
22. Crespo P, Schuebel KE, Ostrom AA, Gutkind JS, Bustelo XR. Phosphotyrosine-dependent activation of Rac-1 GDP/GTP exchange by the vav proto-oncogene product. Nature. 1997;385:169–172.
23. Eva A, Aaronson SA. Isolation of a new human oncogene from a diffuse B-cell lymphoma. Nature. 1985;316:273–275.
24. Habets GG, Scholtes EH, Zuydgeest D, et al. Identification of an invasion-inducing gene, Tiam-1, that encodes a protein with homology to GDP-GTP exchangers for Rho-like proteins. Cell. 1994;77:537–549.
25. Aznar S, Fernandez-Valeron P, Espina C, et al. Rho GTPases: potential candidates for anticancer therapy. Cancer Lett. 2004;206:181–191.
26. Banyard J, Anand-Apte B, Symons M, et al. Motility and invasion are differentially modulated by Rho family GTPases. Oncogene. 2000;19: 580–591.
27. Jaffe AB, Hall A. Rho GTPases in transformation and metastasis. Adv Cancer Res. 2002;84:57–80.
28. Lin M, van Golen KL. Rho-regulatory proteins in breast cancer cell motility and invasion. Breast Cancer Res Treat. 2004;84:49–60.
29. Rosenfeld C, Goutner A, Choquet C, et al. Phenotypic characterisation of a unique non-T, non-B acute lymphoblastic leukaemia cell line. Nature. 1977;267:841–843.
30. Uphoff CC, MacLeod RA, Denkmann SA, et al. Occurrence of TEL-AML1 fusion resulting from (12;21) translocation in human early B-lineage leukemia cell lines. Leukemia. 1997;11:441–447.

31. Morikawa S, Tatsumi E, Baba M, Harada T, Yasuhira K. Two E-rosette-forming lymphoid cell lines. Int J Cancer. 1978;21:166–170.
32. Sambrook J, Fritsch EF, Maniatis T. Molecular Cloning: A Laboratory Manual. 2nd ed. New York: Cold Spring Harbor Laboratory Press; 1989.
33. Hall PA, Levison DA, Woods AL, et al. Proliferating cell nuclear antigen (PCNA) immunolocalization in paraffin sections: an index of cell proliferation with evidence of deregulated expression in some neoplasms. J Pathol. 1990;162:285–294.
34. Ren XD, Kiosses WB, Schwartz MA. Regulation of the small GTP-binding protein Rho by cell adhesion and the cytoskeleton. EMBO J. 1999;18:578–585.
35. Reid T, Furuyashiki T, Ishizaki T, et al. Rhotekin, a putative target for Rho bearing homology to a serine/threonine kinase, PKN and Rhophilin in the Rho binding domain. J Biol Chem. 1996;271: 13556–13560.
36. Gosser YQ, Nomanbhoy TK, Aghazadeh B, et al. C-terminal binding domain of Rho GDP-dissociation inhibitor directs N-terminal inhibitory peptide to GTPases. Nature. 1997;387:814–819.
37. Biou V, Gibrat JF, Levin JM, Robson B, Garnier J. Secondary structure prediction: combination of three different methods. Protein Eng. 1988; 2:185–191.
38. Hordijk PL, ten Klooster JP, Van der Kammen RA, Michiels F, Oomen LCJM, Collard JG. Inhibition of invasion of epithelial cells by Tiam1-Rac signaling. Science. 1997;278:1464–1466.
39. Hotchin NA, Hall A. The assembly of integrin adhesion complexes requires both extracellular matrix and intracellular rho/rac GTPases. J Cell Biol. 1995;131:1857–1865.
40. Tokman MG, Porter RA, Williams CL. Regulation of cadherin-mediated adhesion by the small GTP-binding protein Rho in small cell lung carcinoma cells. Cancer Res. 1997;57:1785–1793.
41. Itoh K, Yoshioka K, Akedo H, Uehata M, Ishizaki T, Narumiya S. An essential part Rho-associated kinase in the transcellular invasion of tumor cells. Nat Med. 1999;5:221–225.
42. Hirao M, Sato N, Kondo T, et al. Regulation mechanism of ERM (ezrin/radixin/moesin) protein/plasma membrane association: possible involvement of phosphatidylinositol turnover and Rho-dependent signaling pathway. J Cell Biol. 1996;135:37–51.
43. Zhang Y, Zhang B. D4-GDI, a Rho GTPase regulator, promotes breast cancer cell invasiveness. Cancer Res. 2006;66:5592–5598.
44. Ishizaki H, Togawa A, Tanaka-Okamoto M, et al. Defective chemokine-directed lymphocyte migration and development in the absence of rho guanosine diphosphate-dissociation inhibitors alpha and beta. J Immunol. 2006;177:8512–8521.
45. Danley DE, Chuang TH, Bokoch GM. Defective Rho GTPase regulation by IL-1 beta-converting enzyme-mediated cleavage of D4 GDP dissociation inhibitor. J Immunol. 1996;157:500–503.
46. Rickers A, Brockstedt E, Mapara MY, Otto A, Dorken B, Bommert K. Inhibition of CPP32 blocks surface IgM-mediated apoptosis and D4-GDI cleavage in human BL60 Burkitt lymphoma cells. Eur J Immunol. 1998;28:296–304.
47. Yin L, Schwartzberg P, Scharton-Kersten TM, Staudt L, Lenardo M. Immune responses in mice deficient in Ly-GDI, a lymphoid-specific regulator of Rho GTPases. Mol Immunol. 1997;34:481–491.
48. Guillemot J-C, Kruskal BA, Adra CN, et al. Targeted disruption of guanosine diiphosphate-dissociation inhibitor for Rho-related protein, GDID4: normal hematopoietic differentiation but subtle defect in superoxide production by macrophages derived from in vitro embryonal stem cell differentiation. Blood. 1996;88:2722–2731.
49. Li S, Ross DT, Kadin ME, Brown PO, Wasik MA. Comparative genome-scale analysis of gene expression profiles in t cell lymphoma cells during malignant progression using a complementary DNA microarray. Am J Pathol. 2001;158:1231–1237.
50. Tapper J, Kettunen E, El Rifai W, et al. Changes in gene expression during progression of ovarian carcinoma. Cancer Genet Cytogenet. 2001;128:1–6.
51. Gildea JJ, Seraj MJ, Oxford G, et al. RhoGDI2 is an invasion and metastasis suppressor gene in human cancer. Cancer Res. 2002;62:6418–6423.
52. Theodorescu D, Sapinoso LM, Conaway MR, et al. Reduced expression of metastasis suppressor RhoGDI2 is associated with decreased survival for patients with bladder cancer. Clin Cancer Res. 2004;10: 3800–3806.

Available online at www.sciencedirect.com
ScienceDirect
Environment International 33 (2007) 1048–1056
ENVIRONMENT INTERNATIONAL
www.elsevier.com/locate/envint

Polybrominated diphenyl ethers and persistent organochlorines in Japanese human adipose tissues

Tatsuya Kunisue [a], Nozomi Takayanagi [a], Tomohiko Isobe [a], Shin Takahashi [a], Masato Nose [b], Taketo Yamada [c], Hiroaki Komori [b], Norimasa Arita [b], Norifumi Ueda [b], Shinsuke Tanabe [a,*]

[a] *Center for Marine Environmental Studies (CMES), Ehime University, Bunkyo-cho 2-5, Matsuyama 790-8577, Japan*
[b] *Department of Pathology, Ehime University School of Medicine, Shitsukawa, Toon 791-0295, Japan*
[c] *Department of Pathology, School of Medicine, Keio University, Shinanomachi 35, Shinjuku-ku 160-8582, Japan*

Received 18 January 2007; accepted 2 June 2007
Available online 25 July 2007

Abstract

The present study determined concentrations of polybrominated diphenyl ethers (PBDEs) and persistent organochlorines (OCs) in Japanese human adipose tissues collected during 2003–2004. Concentrations of PBDEs in adipose tissues were 1–2 orders of magnitude lower than those of OCs. However, observed PBDE congener levels in this study were relatively higher than those in Japanese human adipose tissues collected during 2000 reported previously, while OC levels were comparable to those in specimens collected during 1999 reported by our group. In addition, no age-dependent accumulation of PBDEs was observed, while OC levels except chlordane compounds increased with age. These results indicate recent human exposure to PBDEs in Japan. Among PBDE congeners accumulated in Japanese adipose tissues, BDE-153 was dominant, but this trend was different from those in human milk (BDE-47) and blood (BDE-209) reported previously in Japan, implying the congener-specific kinetics in human bodies. The significant positive correlations between PBDEs and OCs were observed in Japanese adipose tissues, indicating the similar exposure route of these contaminants for Japanese citizens, probably via fish intake.

Keywords: PBDEs; OCs; Human adipose tissue; Japan

1. Introduction

Polybrominated diphenyl ethers (PBDEs), which are in use as brominated flame retardants (BFRs), have been detected in a wide range of animal species due to their bioaccumulative nature (Law et al., 2003), as in the case of persistent organochlorines (OCs). It is highly possible that PBDEs cause adverse effects, such as clinical, morphological, immunological, and behavioral effects, thyroid hormone homeostasis disturbance, and enzyme induction, in animals, already shown based on *in vivo* and *in vitro* studies using experimental mammals and human cell lines (Darnerud, 2003; Gill et al., 2004; Legler and Brouwer, 2003). Therefore, human exposure to PBDEs is of great concern. In Europe and North America, many studies on contamination status of PBDEs in humans have been conducted (Gill et al., 2004); human exposure to PBDEs originating from technical pentaBDE is especially pronounced in North America (Sjödin et al., 2003).

In Japan, technical tetra- and octa-BDE products were used as flame retardants until 1990 and 1999, respectively, and technical deca-BDE is in use even now (Watanabe and Sakai, 2003). These PBDE mixtures were frequently used for television sets manufactured during 1980–1990s and now their disposal is of particular concern (Watanabe and Sakai, 2003). PBDEs have been detected in various Japanese environmental media and biota such as air, sediment, and fish (Watanabe and Sakai, 2003). Hence, investigations on residue levels of PBDEs in Japanese human blood and milk have been recently conducted to assess human exposure to these contaminants (Akutsu et al., 2003; Eslami et al., 2006; Inoue et al., 2006; Takasuga et al., 2004). In a time trend study, it was

* Corresponding author. Tel./fax: +81 89 927 8171.
E-mail address: shinsuke@agr.ehime-u.ac.jp (S. Tanabe).

0160-4120/$ - see front matter © 2007 Elsevier Ltd. All rights reserved.
doi:10.1016/j.envint.2007.06.006

reported that PBDE levels in human milk increased from 1973 to 1998 and then tended to decrease until 2000 (Akutsu et al., 2003). But Eslami et al. (2006) reported higher concentrations of PBDEs in human milk collected during 2004 than in the samples of the year 2000 collected by Akutsu et al. (2003), indicating recent increase in human exposure to these contaminants. In addition, the only study that analyzed tetra–hepta-BDEs in Japanese human adipose tissues showed notably higher concentrations of PBDEs in the specimens collected during 2000 than those of 1970 and the different accumulation patterns between them, suggesting the increased exposure and altered exposure profiles to PBDEs in the past thirty years (Choi et al., 2003). Thus, even though some investigations on contamination status of PBDEs in humans have been conducted, little information on accumulation features such as age- and sex-dependent variations of PBDEs, especially higher brominated congeners such as deca-BDE (BDE209), is available in Japan. Takasuga et al. (2004) reported significantly higher levels of BDE-209 in Japanese human blood compared with tri-hepta-BDE congeners, revealing recent exposure to BDE-209 derived from technical deca-BDE. In addition, it can be anticipated that Japanese people may be exposed to octa–nona-BDE congeners, because these high brominated congeners are abundant in technical octa- and deca-BDE products (La Guardia et al., 2006). To our knowledge, however, no data is available on octa–nona-BDE congeners in human adipose tissue and organs, while a single study has reported concentrations of these high brominated congeners in blood and milk of Japanese women (Inoue et al., 2006).

The present study determined concentrations of di–deca-BDE congeners in Japanese human adipose tissues and examined the congener patterns and sex- and age-dependent accumulations. We also provide information on the most recent status of contamination by persistent OCs such as PCBs, DDTs, HCHs, chlordane compounds (CHLs), and HCB in Japanese people.

2. Materials and methods

2.1. Sample collection

The present study was approved by the Ethics Committee of the Ehime and Keio University Institutional Review Boards. Informed consent was obtained from all the donor's families before sample collection. Adipose tissue (mesenteric fat) samples were collected from 28 donors (male; $n=18$, female; $n=10$) at autopsy during 2003–04. All the samples were stored in the Environmental Specimen Bank (*es*-BANK) for Global Monitoring, Ehime University (Tanabe, 2006) at −20 °C until analysis. The details of cases are shown in Table 1.

2.2. Chemical analysis

Analysis of PBDEs was performed following the procedure described by Ueno et al. (2004) with slight modification. Briefly, 6 g of adipose tissue sample was ground with anhydrous sodium sulfate and extracted in a Soxhlet apparatus with a mixture of hexane and diethyl ether. $^{13}C_{12}$-labeled BDE-15, BDE-28, BDE-47, BDE-99, BDE-153, BDE-154, BDE-183, BDE-197, BDE-207, and BDE-209 were spiked into an aliquot of the extract as internal standards. Lipid in this solution was removed by gel permeation chromatography (GPC) packed Bio-Bead S-X 3 (Bio-Rad Laboratories, USA). The PBDE fraction was concentrated and passed through activated silica gel (Wako-gel S-1: Wako Pure Chemical Industries Ltd., Japan) packed in a glass column with 5% dichloromethane (DCM) in hexane for clean up. $^{13}C_{12}$-labeled BDE-139 was added to the final solution prior to gas chromatograph (GC)-mass selective detector (MSD) analysis. Quantification was performed using a GC (Agilent 6890N)-MSD (Agilent 5973N) for di- to hepta-BDEs, and GC coupled with MS (JEOL GCmate II) for octa- to deca-BDEs, using electron ionization with selective ion monitoring (EI-SIM) mode. GC columns used for quantification were DB-1 (J&W Scientific Inc., USA) having 30 m × 0.25 mm i.d. × 0.25 μm film thickness for di- to hepta-BDEs, and 15 m × 0.25 mm i.d. × 0.1 μm film thickness for octa- to deca-BDEs. Thirteen PBDE congeners (BDE-15, BDE-28, BDE-47, BDE-99, BDE-100, BDE-153, BDE-154, BDE-183, BDE-196, BDE-197, BDE-206, BDE-207 and BDE-209) were quantified in this study. All the congeners were quantified using the isotope dilution method to the corresponding $^{13}C_{12}$-labeled congeners. Recoveries for $^{13}C_{12}$-labeled BDEs were within 60–110%.

OCs including PCBs, DDTs, HCHs, CHLs, and HCB were analyzed following the method described previously (Minh et al., 2001). Another aliquot of the extract was subjected to GPC for lipid removal. The lipid-removed extract was passed through activated Florisil (Florisil PR: Wako chemicals USA, Inc., USA) packed in a glass column. The first fraction eluted with hexane contained PCBs, HCB, *p,p'*-DDE and *trans*-nonachlor, and the second fraction eluted with 20% DCM in hexane contained *p,p'*-DDT, *p,p'*-DDD, HCH isomers (α-, β-, and γ-), *cis*-nonachlor, *trans*-nonachlor, *cis*-chlordane, *trans*-chlordane, oxychlordane. OCs were quantified using a GC (GC column; DB-1, 30 m × 0.25 mm i.d. × 0.25 μm film thickness, J&W Scientific Inc.)-ECD (electron capture detector). The concentration of individual OCs was quantified from the peak area of the samples to that of the corresponding external standard. The PCB

Table 1
Information on the Japanese human adipose samples analyzed in this study

Sample no.	Sex[a]	Age (year)	Clinical diagnosis
1	M	25	Rhabdomyosarcoma
2	M	34	Hepatic insufficiency, hepatitis B
3	M	40	Hepatic insufficiency, renal failure
4	M	41	Liposarcoma, liver metastasis, lung metastasis
5	M	49	Malignant melanoma
6	M	57	Cholangiocarcinoma
7	M	58	Acute myelocytic leukemia
8	M	60	Hepatocellular carcinoma
9	M	66	Renal insufficiency
10	M	69	Cervical lymphnode metastatic cancer of unknown origin
11	M	70	Perforation of gastro-intestinal tract, pneumocystis carini pneumonia
12	M	73	Gastric cancer, malgnant lymphoma
13	M	76	Pneumonia, idiopathic interstitial pneumonia
14	M	79	Lung cancer
15	M	79	Malignant lymphoma
16	M	81	Pancreatic cancer
17	M	81	Metastatic liver cancer
18	M	81	Cardiac infarction
19	F	53	Acute myelocytic leukemia
20	F	59	Acute lymphocytic leukemia
21	F	62	Multiple systemic atrophy
22	F	62	Breast cancer
23	F	69	Carcinoma of the gallbladder
24	F	71	Breast cancer, lymphoangitis carcinomatosa, idiopathic interstitial pneumonia
25	F	72	Hepatic insufficiency, liver cirrhosis associated with HBV infection
26	F	76	Gastric cancer, lung cancer
27	F	83	Lung cancer
28	F	109	Senile deterioration

[a] M; Male, F; Female.

standard used for quantification was an equivalent mixture of 62 PCB isomers (BP-MS; Wellington Laboratories Inc., Canada). Concentrations of individually resolved peaks of PCB isomers were summed up to obtain total PCB concentrations. The recoveries of OCs by this method were 97.0±4.2% for PCBs, 105.0±5.7% for DDTs, 98.9±6.3% for HCHs, 103.9±4.3% for CHLs and 104.1±7.9% for HCB, respectively. Concentrations of PCBs and OC pesticides were not corrected for recovery rates.

Procedural blanks were analyzed simultaneously with every batch of five samples to check for interferences or contamination from solvent and glassware. Lipid contents were determined by measuring the total nonvolatile solvent extractable material on subsamples taken from the original extracts. The concentrations of organohalogens are expressed on lipid weight basis unless otherwise specified.

For quality assurance and quality control, our laboratory participated in the Interlaboratory Comparison Exercise Program for Organic Contaminants in Marine Mammal Tissues organized by the National Institute of Standards and Technology (Gaithersburg, MD, USA) and Marine Mammal Health and Stranding Response Program of the National Oceanic and Atmospheric Administration's National Marine Fisheries Service (Silver Spring, MD, USA). Standard reference material SRM 1945 was analyzed for selected PBDE and PCB congeners, and persistent OC pesticides before the analysis of adipose tissue samples. Reliable results were obtained by comparison of data from our laboratory with those from standard reference values.

2.3. Statistical analysis

The Mann–Whitney *U* test was employed to detect the differences of organohalogen concentrations between males and females. Spearman's rank correlation coefficient was used to measure the strength of the association between age and organohalogen concentrations, and between PBDE and OC concentrations. A p value of less than 0.05 was considered to indicate statistical significance. These analyses were executed using StatView (Version 4.51.1, Abacus Concepts, Inc., USA).

3. Results and discussion

3.1. Residue levels and comparison with other data

Organohalogen compounds were detected in all the human adipose tissue samples analyzed in this study. DDTs (range; 38–3800 ng/g) were dominant, followed by PCBs (90–3100 ng/g)>HCHs (3.5–3800 ng/g)>CHLs (23–730 ng/g)>HCB (1.6–100 ng/g)>PBDEs (1.8–46 ng/g). Concentrations of PBDEs were 1–2 orders of magnitude lower than those of OCs (Tables 2 and 3).

Concentrations of OCs in human adipose tissues analyzed in this study were almost similar to those in the samples collected during 1999, which was reported by our study group (Minh et al., 2001). This indicates that human exposure and accumulation of OCs are in steady-state and these contaminants accumulated in adipose tissues are more stable. To our knowledge, data on PBDEs in Japanese human adipose tissues is available only for women investigated during 2000 (Choi et al., 2003). Although total PBDE levels in adipose tissues observed in this study cannot be compared with those reported by Choi et al. (2003) because of no data on higher brominated congeners such as octa–deca-BDEs, median concentrations of each di–hepta-BDE congener in females analyzed in this study (Table 2) were slightly higher than those (Table 4) detected by Choi et al. (2003). This implies that Japanese people have been recently exposed to relatively high levels of PBDEs. Especially, BDE-153 levels in females observed in this study were about three times higher than data of Choi et al. (2003), indicating specific exposure to this isomer. In Japan, technical hexa-BDE, in which BDE-153 is abundant, was used in the past (Akutsu et al., 2003), and hence Akutsu et al. (2003) suggest human exposure to BDE-153 derived from this technical product.

Some studies on PBDEs in human adipose tissues have been conducted in other countries, but the target PBDE congeners in almost all the studies were BDE-47, BDE-99, BDE-100, BDE-153, and BDE-154. When total concentrations of BDE-47+ BDE-99+ BDE-153, which were analyzed in all the studies, were compared, the observed levels in Japanese adipose tissues were notably lower than those in USA (Johnson-Restrepo et al., 2005; She et al., 2002) and comparable to those in European countries (Covaci et al., 2002; Fernandez et al., 2007; Guvenius et al., 2001; Naert et al., 2006; Smeds and Saukko, 2003) (Table 4). Very little information on higher brominated congeners such as octa–deca-BDEs in human adipose tissues is available worldwide. Johnson-Restrepo et al. (2005) reported that BDE-209 was not detected in adipose tissues of New York citizens. Interestingly, octa–deca-BDE congeners were found in Japanese adipose tissues analyzed in this study. Considering that technical octaBDE was used until 1999 and technical deca-BDE is in use in Japan (Watanabe and Sakai, 2003), it is highly probable that Japanese

Table 2
Concentrations (ng/g lipid wt.) of PBDEs in Japanese human adipose tissues collected during 2003–04

	Male (n=18)			Female (n=10)		
	Mean±SD	Median	(Range)	Mean±SD	Median	(Range)
Age[a]	62±18	68	(25–81)	72±16	70	(53–109)
Lipid (%)	61±17	64	(11–82)	69±10	73	(50–81)
BDE15	0.26±0.24	0.12	(0.017–0.82)	0.17±0.15	0.12	(0.031–0.45)
BDE28	0.32±0.27	0.22	(0.093–0.86)	0.18±0.12	0.17	(0.050–0.39)
BDE47	1.7±1.7	0.84	(0.29–5.9)[b, *]	0.61±0.26	0.70	(0.13–0.94)
BDE99	0.26±0.20	0.21	(0.049–0.65)[b, *]	0.094±0.044	0.099	(0.025–0.15)
BDE100	0.75±0.78	0.39	(0.049–2.5)[b, *]	0.22±0.074	0.26	(0.073–0.29)
BDE153	3.2±3.2	2.4	(0.12–12)[b, *]	1.1±0.44	0.98	(0.69–2.1)
BDE154	0.20±0.16	0.16	(0.011–0.55)[b, *]	0.086±0.030	0.079	(0.052–0.14)
BDE183	0.18±0.16	0.14	(0.018–0.59)[b, *]	0.068±0.024	0.064	(0.038–0.11)
BDE196	0.22±0.28	0.12	(<0.02–0.93)[b, *]	0.050±0.068	0.023	(<0.02–0.21)
BDE197	1.1±1.2	0.65	(0.066–4.8)[b, **]	0.25±0.23	0.25	(0.098–0.44)
BDE206	0.12±0.19	0.071	(<0.03–0.85)[b, *]	0.036±0.030	0.040	(<0.03–0.089)
BDE207	0.83±1.0	0.47	(0.044–4.4)[b, *]	0.23±0.10	0.22	(0.088–0.40)
BDE209	1.9±2.9	1.2	(<0.5–12)	0.61±0.59	0.74	(<0.5–1.7)
∑ PBDEs	11±11	8.0	(1.8–46)[b, **]	3.7±1.3	3.5	(1.8–6.0)

SD = standard deviation. The concentrations below detection limit were treated as zero for arithmetic mean and median values.
[a] Years. [b] Concentrations in males were significantly higher than those in females. *p<0.05, **p<0.01.